AD-A136 057 FRACTURE BEHAVIOR UNDER IMPACT(U) FRAUNHOFER-INST FUER WERKSTOFFMECHANIK FREIBURG (GERMANY F R) J F KALTHOFF ET AL. JUL 83 W-11/83 DAJA37-81-C-0013 1/1

UNCLASSIFIED F/G 20/11 NL

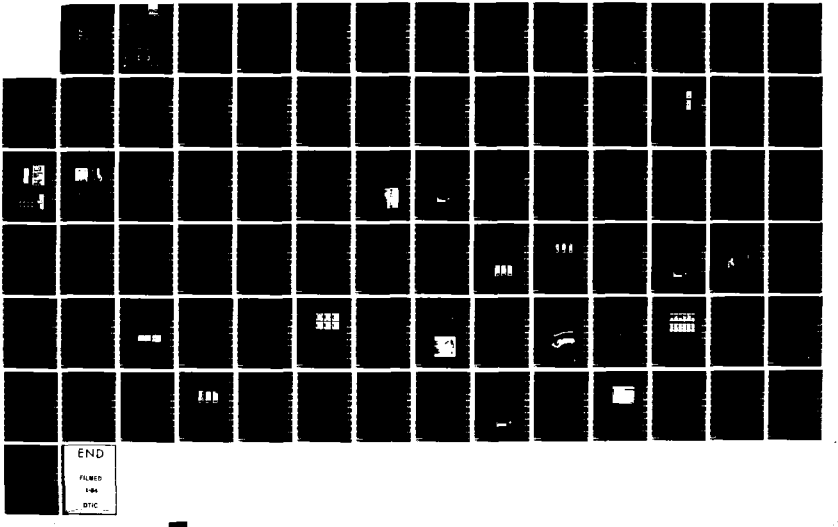

END

FILMED

1-84

DTIC

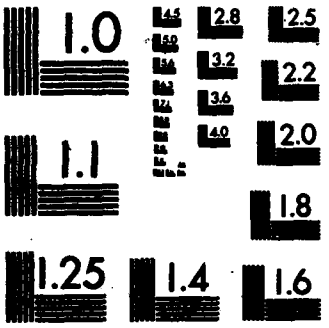

MICROCOPY RESOLUTION TEST CHART
NATIONAL BUREAU OF STANDARDS-1963-A

FhG

Fraunhofer-Gesellschaft

FRACTURE BEHAVIOR UNDER IMPACT

W 11/83

3rd Semi-Annual Progress Report

by

J.F. Kalthoff and S. Winkler

Reporting Period Feb. 1983 - July 1983

Fraunhofer-Institut
für Werkstoffmechanik

UNCLASSIFIED

SECURITY CLASSIFICATION OF THIS PAGE (When Data Entered)

R&D 3012-MS

REPORT DOCUMENTATION PAGE	READ INSTRUCTIONS BEFORE COMPLETING FORM
1. REPORT NUMBER	2. GOVT ACCESSION NO. AD-A136057	3. RECIPIENT'S CATALOG NUMBER
4. TITLE (and Subtitle) Fracture Behavior Under Impact	5. TYPE OF REPORT & PERIOD COVERED 3rd Semi-Annual Progress Report
	6. PERFORMING ORG. REPORT NUMBER
7. AUTHOR(s) J.F. Kalthoff and S. Winkler	8. CONTRACT OR GRANT NUMBER(s) DAJA37-81-C-0013
9. PERFORMING ORGANIZATION NAME AND ADDRESS Fraunhofer-Institut für Werkstoffmechanik Wöhlerstr 11, 7800 Freiburg/Brsg West Germany	10. PROGRAM ELEMENT, PROJECT, TASK AREA & WORK UNIT NUMBERS 6.11.02A T161102BH57-06
11. CONTROLLING OFFICE NAME AND ADDRESS USARDSG-UK Box 65 FPO NY 09510	12. REPORT DATE FEB 83 - JUL 83
	13. NUMBER OF PAGES 74
14. MONITORING AGENCY NAME & ADDRESS(if different from Controlling Office)	15. SECURITY CLASS. (of this report) Unclassified
	15a. DECLASSIFICATION/DOWNGRADING SCHEDULE

16. DISTRIBUTION STATEMENT (of this Report)

Approved for public release; distribution unlimited

Accession For	
NTIS GRA&I	☑
DTIC TAB	☐
Unannounced	☐
Justification	
By	
Distribution/	
Availability Codes	
Dist	Avail and/or Special
A1	

17. DISTRIBUTION STATEMENT (of the abstract entered in Block 20, if different from Report)

18. SUPPLEMENTARY NOTES

DTIC COPY INSPECTED

19. KEY WORDS (Continue on reverse side if necessary and identify by block number)

Multiple cracks, high strength steel, high speed photography, dynamic stress, dynamic fracture toughness, fracture toughness.

20. ABSTRACT (Continue on reverse side if necessary and identify by block number)

The physical behavior of cracks under impact loading is investigated. Single edge cracks or arrays of multiple cracks in rectangular specimens are considered. The specimens are loaded by time dependent tensile stress pulses moving perpendicular to the crack direction. The specimens are either directly loaded by an impinging projectile or by a base plate which is accelerated by the projectile. The specimens are made from a transparent model material or a high strength steel. The initial crack lengths and impact velocities are varied

DD FORM 1 JAN 73 1473 EDITION OF 1 NOV 65 IS OBSOLETE

UNCLASSIFIED

SECURITY CLASSIFICATION OF THIS PAGE (When Data Entered)

20) throughout the experiments. Utilizing the shadow optical method of caustics in combination with high speed photography , the dynamic stress intensity factors at the tip of the crack are measured as functions of time during the impact event. The critical value of the dynamic stress intensity factor at onset of rapid crack propagation, i.e. the dynamic fracture toughness K_{Id}, is determined and discussed with regard to the times t_f at which the crack becomes unstable. The results are compared with corresponding static fracture toughness data.

FRAUNHOFER-INSTITUT FOR WERKSTOFFMECHANIK
Wöhlerstr. 11, D-7800 Freiburg

FRACTURE BEHAVIOR UNDER IMPACT

W 11/83

3rd Semi-Annual Progress Report

by

J.F. Kalthoff and S. Winkler

Reporting Period Feb. 1983 - July 1983

United States Army
EUROPEAN RESEARCH OFFICE OF THE U.S. Army
London England

CONTRACT NUMBER DAJA 37-81-C-0013

The Research reported in this document has been made possible through the support and sponsorship of the U.S. Government through its European Research Office of the U.S. Army. This report is intended only for the internal managment use of the Contractor and the U.S. Government.

1. TECHNICAL OBJECTIVES

The physical behavior of cracks under impact loading is investigated. Single edge cracks or arrays of multiple cracks in rectangular specimens are considered. The specimens are loaded by time dependent tensile stress pulses moving perpendicular to the crack direction. The specimens are either directly loaded by an impinging projectile or by a base plate which is accelerated by the projectile. The specimens are made from a transparent model material or a high strength steel. The initial crack lengths and impact velocities are varied throughout the experiments. Utilizing the shadow optical method of caustics in combination with high speed photography, the dynamic stress intensity factors at the tip of the crack are measured as functions of time during the impact event. The critical value of the dynamic stress intensity factor at onset of rapid crack propagation, i.e. the dynamic fracture toughness K_{Id}, is determined and discussed with regard to the times t_f at which the crack becomes unstable. The results are compared with corresponding static fracture toughness data.

2. STATEMENT OF WORK

The investigations carried out in the second year have been continued during the first half of the third year, i.e. this reporting period. In particular experiments on the mutual interaction of cracks under dynamic loading have been performed to support earlier results, described in the Second Annual Report. This work has been completed. More experiments have been performed to investigate the fracture behavior of single edge cracks under direct impact loading conditions. In these experiments higher impact velocities have been applied than in the experiments carried out before (see Second Annual Report). These data supplement existing data into the lower time to fracture regime. Results obtained on these two topics have been reported in the paper "On some Current Problems in Experimental Fracture Dynamics", by J.F. Kalthoff, presented at the "Workshop on Dynamic Fracture", sponsored by NSF and ARO, organized by W.G. Knauss, California Institute of Technology, Pasadena, Calif. Februar 17-18, 1983. A copy of the paper is attached to this Report in the Annex.

The investigation of dynamic fracture in metal specimens has begun. Previous shadow optical investigations have been performed with specimens made from the high strength steel X 2 NiCoMo 18 9 5 (which is similar to the American designation 18 Ni maraging grade 300). Since this steel is very expensive studies have been performed with other metals of practical interest: A high strength aluminum and a high strength steel, both used for armor purposes, have been utilized. The shadow optical technique yielded satisfactory results with both metals although the plastic zones at the crack tips were considerable larger than for the steel X 2 NiCoMo 18 9 5. A plate of the investigated armor steel has been made available for subsequent investigations by Mr. H. Senf, Fraunhofer-Institut für Kurzzeitdynamik, Ernst-Mach-Institut, Abteilung für Ballistik, Weil am Rhein. First impact experiments have been performed with steel specimens applying the shadow optical technique in reflection. The results indicate that the arrangement has to be very carefully aligned. Slight deviations from a straight impact result in deformations of the specimen surfaces which cause significant disturbances of the caustics. Subsequent experiments have been successfull and showed undisturbed caustics. In order to safe specimen material a series of experiments has been performed to find the smallest possible specimen dimensions which yield accurate results. As already reported in the First Annual Report difficulties due to crack path deviations arise if the specimens are too small. About 300 mm was found to be the smallest acceptable specimen length.

In addition to tensile loading of cracks a few experiments have been performed under dynamic bending. In the direct loading arrangement (see Fig. 5 of the Second Annual Report) the specimen was rotated by 90^{0} and tested as a pre-cracked bend specimen. Other investigations performed at IWM have shown that notched bend specimens under drop weight loading lose contact with the supports during the early phase of the impact process. During this loss-of-contact phase specimen failure has been observed in many experiments. Since at high loading rates the specimens will fail even earlier it is natural that a high rate bend test can be carried out with unsupported specimens, i.e. in a one-point-bend arrangement. Results of dynamic one-point-bend experiments have been reported in the paper "Mechanical Response of Cracks to Impact Loading", presented at the International Conference on

"Dynamic Mechanical Properties and Fracture Dynamics of Engineering Materials", organized by Z. Bilek, Czechoslovak Academy of Sciences, Institute of Physical Metallurgy, Brno-Valtice CSSR, June 16-18, 1983 and in the paper "Time effects and their Influences on Test Procedures for Measuring Dynamic Material Strength Values", presented at the International Conference on the "Application of Fracture Mechanics to Structures and Materials", Freiburg, June 20-27, West Germany. Copies of the two papers are attached to this Report in the Annex.

3. NEXT STEPS

The experiments with high strength steel specimens performed under direct impact loading conditions will be continued. Since this material is more strain rate sensitive than the model material Araldite B and since higher impact velocities can be applied in these experiments, more informative data on the dependence of the impact fracture toughness from loading rate are expected.

ANNEX

WORKSHOP ON DYNAMIC FRACTURE

Sponsored by the National Science Foundation and
the Army Research Office

J.F. KALTHOFF, Institut für Werkstoffmechanik,
"On Some Current Problems in Experimental Fracture Dynamics"

February 17 and 18, 1983
California Insitute of Technology
Pasadena, California.

ON SOME CURRENT PROBLEMS IN EXPERIMENTAL FRACTURE DYNAMICS

J.F. Kalthoff
Fraunhofer-Institut für Werkstoffmechanik,
Wöhlerstr. 11, 7800 Freiburg/Brsg., West-Germany
Telefon: 0761/51420

1. INTRODUCTION

The term fracture dynamics includes both, crack tip motion effects and dynamic loading of cracks. Based on the research work at the Fraunhofer-Institut für Werkstoffmechanik (IWM) several topics are discussed regarding the subjects (see Fig. 1): crack propagation, arrest of fact running cracks, time dependent loading in general, and loading of cracks by sharp stress pulses of short duration. Following the guidelines of the workshop, previous results are briefly summarized to state the current situation, but special consideration is given to still open questions and not yet resolved problems.

2. EXPERIMENTAL TECHNIQUE

Most experimental data reported in this paper have been generated by means of the shadow optical method of caustics. The caustic technique is an optical tool for measuring stress intensifications. The method has been applied very successfully in the field of fracture mechanics for determining stress intensity factors. Crack tip caustics are of a simple form and can easily be evaluated. The technique, therefore, is very well suited for investigating complex fracture problems, as for example in fracture dynamics.

The physical principle of the shadow optical method of caustics is illustrated in Fig. 2. A precracked specimen under load is illuminated

by a parallel light beam. A cross-section through the specimen at the crack tip is shown in Fig. 2b for a transparent specimen, and in Fig. 2c for a non-transparent steel specimen. Due to the stress concentration the physical conditions at the crack tip are changed. For transparent specimens both the thickness of the specimen and the refractive index of the material are reduced. Thus, the area surrounding the crack tip acts as a divergent lens and the light rays are deflected outwards. As a consequence, on a screen (image plane) at a distance z_0 behind the specimen a shadow area is observed which is surrounded by a region of light concentration, the caustic (see Fig. 3a). Figure 2c shows the situation for a non-transparent steel specimen with a mirrored front surface. Due to the surface deformations, light rays near the crack tip are reflected towards the center line. An extension of the reflected light rays onto a virtual image plane at the distance z_0 behind the specimen results in a light configuration which is similar to the one obtained in transmission. Consequently a similar caustic is obtained. In Fig. 3b experimentally observed caustics are shown which were photographed in transmission and in reflection with different materials.

The method of caustics was introducted by Manogg [1,2] in 1964. Later on, Theocaris [3] further developed the technique. The author and his coworkers extended and applied Manogg's method for investigating dynamic fracture phenomena [4-7]. For further details of the technique see [8,9].

3. DYNAMIC CRACKS

In this chapter dynamic effects associated with crack tip motion are discussed.

3.1. Crack Propagation

The stress intensification and the path stability of dynamically propagating cracks are considered in the following two sections.

3.1.1. Stress intensity - crack velocity - relationship

Data on the dynamic stress intensity factor as a function of crack velocity (K-v-curve) have been obtained by the author and his colleagues from many crack arrest experiments with various types of specimens made

from the model material Araldite B (see Fig. 4, and [4,5,10]). All data lie within a broad band. Large scatter is observed for each type of specimen, but a tendency for lower or higher values is observed when different types of specimens are considered. The large variations in stress intensity for the same crack velocity could be due to modifications in the experimental conditions, which were unavoidable in the course of the investigations (e.g. due to different batches of material). Therefore, experiments were carried out under practically identical conditions with DCB- and SEN-specimens (see Fig. 5). Two clearly seperated K-v-curves were obtained, the one for the DCB-specimen showing significantly higher (up to 20 %) values than the one for the SEN-specimen. Additional experiments with a DCB/SEN-combination specimen (see insert in Fig. 6) confirmed these differences: Data measured in the DCB-section of the specimen fell on the previously measured curve for the DCB-specimen, and accordingly for the SEN-section. It must be speculated, therefore, that K-v-curves are not unique, but dependent on specimen geometry. Kobayashi et al. [11] and Dally et al. [12] measured similar data for the material Homalite 100 by means of photo-elastic techniques (Figs. 7 and 8). Kobayashi concludes that the scatter in the data are an indication of the non-uniqueness of K-v-curves. Dally [12], however, argues that the different results are due to insufficiencies of the current data evaluation procedures and speculates that the K-v-relationship, in particular the stem of the curve, is unique.

In the following paragraph it is assumed for the moment that K-v-curves ar <u>not unique</u>. In order to discuss consequences of this assumption it is worthwhile to introduce and to distinguish between the following two quantities: the dynamic stress intensity factor K_I^{dyn}, i.e. a pure stress field quantity and the dynamic fracture toughness K_{ID}, i.e. a material property. In an energy consideration, K_I^{dyn} represents a measure of the energy which is available at the crack tip, whereas K_{ID} represents a measure of the energy which is actually consumed at the crack tip for propagation. Experimental techniques as shadow optics or photoelasticity measure the stress intensity factor, K_I^{dyn}. The above discussion on the uniqueness or non-uniqueness, therefore, first of all, applies for K_I^{dyn}-v-curves. Thus, it is very well possible, that the

dynamic fracture toughness $K_{ID}(v)$ is nevertheless represented by a unique curve. As a consequence, it would be necessary, however, to assume that the two quantities K_I^{dyn} and K_{ID} can take different values. $K_{ID}(v)$ could be the lower bound of all possible $K_I^{dyn}(v)$-curves, $K_{ID}(v) \leq K_I^{dyn}(v)$ (see schematic representation in Fig. 9). This would imply that more energy can be available at the tip of the propagating crack than is actually absorbed by the propagating crack.

The speculation of an imbalance between the dynamic stress intensity factor K_I^{dyn} and the dynamic fracture toughness K_{ID} raises several questions: Is a single parameter (K) description adequate for dynamic fracture problems? Can there be different results if procedures for determining the dynamic stress intensity factor are based on different approaches: a localized consideration of information obtained from a confined area around the crack tip (experimental techniques) or a global consideration of total energy changes in the whole specimen (numerical techniques)? Are there retardation effects if information at finite observation distances ahead of the crack tip is utilized for determining the dynamic stress intensity factor? (See contribution of L.B. Freund, this volume.)

More theoretical and experimental investigations are necessary to clarify these points. Experiments have been performed by the author and his colleagues [13] to simultaneously measure both quantities, the dynamic stress intensity factor, K_I^{dyn}, and the dynamic fracture toughness, K_{ID}, by two different techniques (see Fig. 10). The shadow optical technique was applied for determining K_I^{dyn}, and temperature measurements were performed to determine the heat production at the tip of the propagating crack, which is a measure of the energy consumption [14] and hence of the dynamic fracture toughness K_{ID}. Preliminary results obtained from experiments with high strength steel specimens are shown in Fig. 11. All data lie within a large scatter band, but there is a tendency for $K_I^{dyn} > K_{ID}$ at high crack velocities. More measurements with improved accuracy are needed and are currently performed to get more definite results.

After this discussion based on the assumption that K-v-curves are not unique it shall be assumed now that K-v-curves are unique. This would imply that the experimental techniques are insufficient to resolve the uniqueness. In principal, the accuracy of evaluation procedures which utilze information at finite distances away from the crack tip can be improved by incorporating higher order terms of the stress field around the crack tip. Work is carried out at IWM in cooperation with colleagues from the University of Maryland to study the effects of higher order terms on the K-determination by caustics. The resulting changes in shape and size of caustics are shown in Fig. 12. Information on the absolute magnitude of the higher order coefficients is necessary to give quantitative estimates on the conditions under which a one parameter K-evaluation yields data of sufficient accuracy. The influences of higher order terms in general are considered to be less severe in shadow optics than in photoelasticity.

More fundamental research is needed to resolve the uncertainties regarding the uniqueness or non-uniqueness of K-v-curves.

3.1.2. Crack path

The crack propagation direction in brittle materials is controlled by the mixed mode stress intensity factors K_I and K_{II} [15,16]; the directional stability is determined by the sign of the second order coefficient a_2 [17]. The formation of a definite crack branching angle (see Fig. 13) is an example of crack propagation in such a direction that pure mode I loading results: As was found by the author [18], the crack tip stress fields of the branches interact with each other, leading to a mixed mode loading. The mode-II stress intensity factor varies in magnitude and changes sign when different branching angles are considered. Accordingly, branches with large/small angles attract/repel each other, and only for a critical branching angle crack propagation in the preexisting direction is possible.

The crack propagation path in bend specimens, in particular under impact loading, shows another interesting feature (see Fig. 14). When the crack approaches the rear end of the specimen it slows down and the following crack path shows a characteristic S-shaped deviation from the original direction. High speed photoelastic investigations (see Fig. 15, [19])

reveal a change from forward loops to backward loops, which occurs prior to the actual change in the crack propagation direction. (see Fig. 15, photographs for times > 420 μs). Backward loops are an indication of a positive value of the second order coefficient a_2. Thus instability of crack propagation direction is expected according to Cotterell's theory [17]. Caustic investigations some time later, when the crack has reached almost zero crack velocity, show a mixed mode loading (see Fig. 16, [7]) which then initiates the change in the crack propagation direction. This problem is investigated further by studying the effect of stress wave interaction with the propagating crack.

3.1.3. Crack arrest

Stress wave effects were also found to have a significant influence on the crack arrest process. Shadow optical investigations have shown (see Fig. 17, [4,5]): At the beginning of the crack propagation event the dynamic stress intensity factor K_I^{dyn} is smaller than the stress intensity factor of an equivalent stationary crack, $K_I^{dyn} < K_I^{stat}$. This is due to elastic waves which are generated by the propagating crack. Kinetic energy is radiated into the specimen. At the end of the crack propagation event, in particular at arrest $K_I^{dyn} > K_I^{stat}$, since waves after reflection at the finite boundaries of the specimen interact with the crack (see Fig. 18) and contribute to the stress intensity factor. Only after arrest, the dynamic stress intensity factor K_I^{dyn} approaches the equivalent static stress intensity factor at arrest, K_{Ia}^{stat}, via an occillation with damped amplitude. The wave effects during the run-arrest event initiate a vibration of the total specimen. The observed experimental findings confirm the Battelle concept of recovered kinetic energy [20,21].

Thus, a statically determined crack arrest toughness K_{Ia}^{stat} can not represent a true material property. Only a dynamically determined crack arrest toughness, K_{Ia}^{dyn} or K_{Im} [5,21], can reflect the true arrest behavior of the material. However, since dynamic effects in large scale structures in general are smaller than in the relatively small laboratory test specimens, static crack arrest analyses will yield conservative safety predictions [22]. On the basis of this understanding the static

crack arrest concept can be applied by the practical engineer. Crack arrest safety analyses would be more widely used in practice if a standardized procedure for measuring the crack arrest toughness K_{Ia} would have been released by ASTM already.

In order to minimize errors in the static crack arrest concept resulting from neglected dynamic effects a RDE-(reduced dynamic effects)-specimen has been developed at IWM (see Figs. 19 and 20). Edges and boundary of the specimen were shaped to reduce wave reflection and to defocus reflected waves. Damping material and additional weights are attached to the "wings" of the specimen to absorb kinetic energy and to increase the period of the eigenoscillation of the specimen in order to reduce the recovery of kinetic energy. Statically determined crack arrest toughness values K_{Ia}^{stat} are shown in Fig. 21 for the RDE-specimen in comparison to data obtained with other crack arrest specimens. The dependence on crack jump distance is about three to four times smaller for RDE-specimens than for the most commonly used C-specimen.

4. DYNAMIC LOADING OF CRACKS

The fracture behavior of cracks under time dependent loads in general is discussed in the following chapter. The loading times are assumed to be considerably larger than the time it takes waves to travel the distance given by the crack length. Effects resulting for shorter load durations are discussed in a seperate chapter.

4.1. Time Dependent Loading

4.1.1. Stationary cracks

A procedure [23] has been proposed to ASTM for measuring the impact fracture toughness K_{Id} of steels with precracked Charpy specimens. The procedure assumes that dynamic stress intensity factors can be determined from loads registered at the tup of the striking hammer via a static analysis, if the times of interest are larger than three times the period τ of the eigenoscillation of the specimen (see Fig. 22). A comparison of such stress intensity factors, denoted K_I^{stat}, with the actual dynamic

stress intensity factors, K_I^{dyn}, determined by shadow optics, is shown in Fig. 23, [6]. The results were obtained with specimens of enlarged size made from Araldite B or a high strength steel, tested under drop weight loading at 0.5 m/s. Marked differences were measured between K_I^{stat} and K_I^{dyn}, even for times $t > 3\tau$. Furthermore, such large times to fracture could only be obtained by utilizing low impact velocities. The specimen behavior was investigated further by also measuring the specimen reaction at the anvils [24]. Figure 24 compares the load measured at the striking hammer (a), the stress intensity factor measured at the crack tip (b), the load measured at the anvils (c), and the position of the specimen ends with regard to the anvils (d). The late registration of loads at the anvil results from a loss of contact between the specimen ends and the anvils. This loss of contact can later occur for a second time and loss of contact can also take place between the hammer and the specimen (see Fig. 25). These effects demonstrate the strong influence of inertial effects during impact loading. It is concluded, therefore, that the determination of reliable impact fracture toughness values K_{Id} at reasonably high loading rates does require a fully dynamic evaluation procedure.

Therefore, the author and his colleagues developed the dynamic concept of impact response curves (see Fig. 26, and [25]): For fixed test conditions (i.e. specimen geometry, hammer mass, impact velocity, etc.) the dynamic stress intensity factor versus time relationship is determined by means of the shadow optical method of caustics with a high strength steel specimen. The K_I^{dyn}-t-curve (impact response curve) applies for all steels provided the conditions for small scale yielding are fulfilled. In the real test-experiment with the steel to be investigated, then, only the time to fracture is measured (e.g. by an uncalibrated strain gage near the crack tip). This time together with the preestablished impact response curve determines the impact fracture toughness value K_{Id}. This procedure has been applied successfully with two structural steels (see Fig. 27) impacted at 5 m/s. Although fracture occured at about $0.5\,\tau$ only, the concept of impact response curves gave reliable data.

Work is continued to extend this technique to increased loading rates. Data at loading rates sufficiently higher than those obtained in drop

weight experiments allow to discriminate between the following behavior: the existence of a minimum fracture toughness, a continuous decrease or a final increase of toughness with increasing loading rate (see Fig. 28). Experiments were performed with a gas gun by firing a projectile against a precracked SEN-specimen (see Fig. 29). After reflection of compressive stress waves at the free ends of the specimen the crack is loaded in tension (Fig. 30). Shadow optical analyses indicate dynamic fracture toughness values K_{Id} which are equal to or larger than the static fracture toughness K_{Ic} (see Fig. 31). A toughness increase with increasing loading rate, i.e. with decreasing time to fracture, was also observed by Ravi Chandar and Knauss [26] with PMMA-specimens loaded by electromagnetic techniques (see Fig. 32). Such a behavior can be explained by assuming the existense of an incubation time (see Fig. 33): According to this assumption the crack tip would have to experience a supercritical stress intensity factor for a constant (very likely material related) minimum time before onset of rapid crack propagation can occur. More data at varying loading rates are necessary to verify this assumption.

4.1.2. Interaction of multiple cracks

Due to mutual interaction, the stress intensity factors K_I of two parallel cracks under static loading condition are smaller than the stress intensity factor for an equivalent single crack. In addition a superimposed mode II loading results (see Fig. 34). Experiments were carried out to study the interaction of two parallel cracks under stress pulse loading (see Fig. 35). Shadow optical photographs and the resulting quantitative data are shown in Figs. 36 and 37, [27]. At very early times the crack which is hit by the tensile pulse first shows a similar behavior as the single crack, and the second crack is only less loaded. Some time later, however, the situation changes and the second crack exhibits the larger stress intensity factor. This process varies periodically. At larger times the average stress intensity factor of the parallel cracks is smaller than the one of the single crack, similar as in the static case. This behavior is of significance for the fracture behavior of multiple crack configurations under dynamic loading conditions.

4.1.3. Propagating cracks

Problems are more complex for propagating cracks under time dependent loading. Kanninen et al. [28,29] analysed the crack initiation and crack propagation behavior in precracked bend specimens under quasistatic and under impact loading conditions (see Fig. 38). Dynamic fracture toughness values $K_{ID}(v)$ inferred from these tests were roughly a factor of two different [29]. This finding relates to the question of the uniqueness or non-uniqueness of K-v-curves and would be of great significance for the relevance of safety considerations based on impact test data. The problem is addressed and further clarified in the contribution of M.F. Kanninen, this volume.

4.2. Short Pulse Loading

The author and his colleagues at SRI-International studied the fracture behavior of cracks loaded by stress pulses of durations which are comparable or even smaller than the time it takes waves to travel the distance given by the crack length [30-32]. If the pulse duration is decreased below a certain limit a stress intensity factor according to a simple $\sigma_0\sqrt{\pi a_0}$-relationship does not apply anymore. Instead the behavior is controlled by a rather complex stress intensity history [30]. The stress intensity increases with time to a maximum value which is reached at the end of the pulse, the stress intensity factor then drops off again. The maximum value is $\sigma_0\sqrt{\pi a_{eff}}$, with $a_{eff} \approx c \cdot T_0$, and $a_{eff} < a_0$. T_0 is the pulse duration, c is a wave speed. Assuming that the crack has to experience a supercritical stress intensity factor for at least a certain minimum time in order to become unstable a short pulse fracture criterion was developed. According to this criterion and the stress intensity history discussed above, higher critical stresses are predicted to bring a crack to instability than in the equivalent static case. Furthermore, the instability stresses should not depend on crack length. The general instability behavior of cracks with different lengths subjected to different loading conditions, i.e. pulse amplitude and pulse duration, is shown in a three dimensional (σ_0-a_0-T_0)-diagram,

see Fig. 39, [30]. The short pulse fracture behavior is represented in the rear right section of the diagram, the front left regime (long pulse durations, short crack length) shows the usual static behavior. Short pulse fracture experiments were performed by Shockey et al. [31,32]. Cracks of different lengths in various materials were subjected to stress pulses of different durations (see Figs. 40 and 41, and contribution of D.A. Shockey et al., this volume). The good agreement with the theoretical predictions demonstrates the applicability of the developed short pulse fracture criterion.

5. CONCLUSIONS

Several different problems in the field of fracture dynamics have been discussed. In many cases the physical principles which control the dynamic event are well understood. So it is evident that dynamic processes as crack arrest, impact loading of cracks, short pulse loading of cracks, can only be accurately described by dynamic analyses. Static procedures can lead to erroneous results and are applicable only with restrictions. Some fundamental problems in fracture dynamics, e.g. the energy transfer at the tip of propagating cracks, the crack path stability, the applicability of a single parameter (K) description, the influence of far field effects, etc., seem to need further clarification from both, the theoretical and the experimental point of view.

REFERENCES

1. Manogg, P., "Anwendung der Schattenoptik zur Untersuchung des Zerreißvorgangs von Platten", Dissertation, Universität Freiburg, Germany, 1964.

2. Manogg, P., "Schattenoptische Messung der spezifischen Bruchenergie während des Bruchvorgangs bei Plexiglas", Proceedings, International Conference on the Physics of Non-Crystalline Solids, Delft, The Netherlands, 1964, pp. 481-490.

3. Theocaris, P.S., "Local Yielding Around a Crack Tip in Plexiglas", J. Appl. Mech., Vol. 37, 1970, pp. 409-415.

4. Kalthoff, J.F., Beinert, J., and Winkler, S., "Measurements of Dynamic Stress Intensity Factors for Fast Running and Arresting Crack in Double-Cantilever-Beam-Specimens", ASTM STP 627 - Fast Fracture and Crack Arrest, American Society for Testing and Materials, Philadelphia, U.S.A., 1977, pp. 161-176.

5. Kalthoff, J.F., Beinert, J., Winkler, S., and Klemm, W., "Experimental Analysis of Dynamic Effects in Different Crack Arrest Test Specimens", ASTM STP 711 - Crack Arrest Methodology and Applications, American Society for Testing and Materials, Philadelphia, U.S.A., 1980, pp. 109-127.

6. Kalthoff, J.F., Böhme, W., Winkler, S., and Klemm, W., "Measurements of Dynamic Stress Intensity Factors in Impacted Bend Specimens", CSNI Specialist Meeting on Instrumented Precracked Charpy Testing, EPRI, Palo Alto, Calif., U.S.A., Dec. 1980.

7. Kalthoff, J.F., Böhme, W., and Winkler, S., "Analysis of Impact Fracture Phenomena by Means of the Shadow Optical Method of Caustics", VIIth Intl. Conf. Experimental Stress Analysis, Society for Experimental Stress Analysis, Haifa, Israel, Aug. 23-27, 1982.

8. Beinert, J. and Kalthoff, J.F., "Experimental Determination of Dynamic Stress Intensity Factors by Shadow Patterns" in Mechanics of Fracture, Vol. 7, Ed. G.C. Sih, Martinus Nijhoff Publishers, The Hague, Boston, London, 1981, pp. 281-330.

9. Kalthoff, J.F., "Stress Intensity Factor Determination by Caustics", Intl. Conf. Experimental Mechanics, Society for Experimental Stress Analysis and Japan Society of Mechanical Engineers, Honolulu, Maui, Hawaii, U.S.A., May 23-28, 1982.

10. Kalthoff, J.F., Beinert, J., and Winkler, S., "Influence of Dynamic Effects on Crack Arrest", Draft of Final Report prepared for Electric Power Research Institute, Palo Alto, Calif. under Contract No. RP 1022-1, IWM-Report W 4/80, Freiburg, 1980.

11. Kobayashi, A.S., and Mall, S., "Dynamic Fracture Toughness of Homalite-100", Experimental Mechanics, Vol. 18, No. 1, January 1978, pp. 11-18.

12. Kobayashi, T., Dally, J.W., and Fourney, W.L., "Influence of Specimen Geometry on Crack Propagation and Arrest Behavior, VIth Intl. Conf. Experimental Stress Analysis, Society for Experimental Stress Analysis, München, Germany, Sept. 18-22, 1978.

13. Shockey, D.A., Kalthoff, J.F., Klemm, W., and Winkler, S., "Simultaneous Measurements of Stress Intensity and Toughness for Fast Running Cracks in Steel", to appear in Experimental Mechanics, 1983.

14. Wells, A.A., "The Mechanics of Notch Brittle Fracture", Welding Res. Vol. 7, 1953, pp. 34r-56r.

15. Erdogan, F., and Sih, G.C., "On the Crack Extension in Plates under Plane Loading and Transverse Shear", J. Basic Engng., Trans. ASME, 85 D, 1983, pp. 519-525.

16. Kerkhof, F., "Wave Fractographic Investigations of Brittle Fracture Dynamics", Proc. Intl. Conf. Dynamic Crack Propagation, Ed. G.C. Sih, Lehigh University, Bethlehem, Pa., U.S.A., July 10-12, 1972.

17. Cotterell, B., "Notes on the Paths and Stability of Cracks", Intl. J. Fracture, Vol. 2, 1966, pp. 526-533.

18. Kalthoff, J.F., "On the Propagation Direction of Bifurated Cracks", Proc. Intl. Conf. Dynamic Crack Propagation, Ed. G.C. Sih, Lehigh University, Bethlehem, Pa., U.S.A., July 10-12, 1982.

19. Böhme, W., and Kalthoff, J.F., "Untersuchungen des Bruchverhaltens schlagbelasteter Dreipunktbiegeproben unter Einsatz verschiedener Meßverfahren der Spannungsanalyse", 15. Sitzung, Arbeitskreis Bruchvorgänge im Deutschen Verband für Materialprüfung, Darmstadt, Febr. 22-23, 1983 and 7th Symposium, Gemeinschaft Experimentelle Spannungsanalyse, Schliersee, May 2-3, 1983.

20. Hahn, G.T., Hoagland, R.G., Kanninen, M.F., and Rosenfield, A.R., "A Preliminary Study of Fast Fracture and Arrest in the DCB Test Specimen", Proc. Intl. Conf. Dynamic Crack Propagation, Ed. G.C. Sih, Lehigh University, Bethlehem, Pa., U.S.A., July 10-12, 1972.

21. Hahn, G.T., Gehlen, P.C., Hoagland, R.G., Kanninen, M.F., Rosenfield, A.R. et al., "Critical Experiments, Measurements and Analyses to Establish a Crack Arrest Methodology for Nuclear Pressure Vessel Steels," BMI-1937, 1959, 1995, Battelle Colombus Laboratories, Columbus, Ohio, Aug. 1975, Oct. 1976, May 1978.

22. Kalthoff, J.F., Beinert, J., and Winkler, S., "Einfluß dynamischer Effekte auf die Bestimmung von Rißarrestzähigkeiten und auf die Anwendung von Rißarrestsicherheitsanalysen", 8. Sitzung, Arbeitskreis Bruchvorgänge im Deutschen Verband für Materialprüfung, Köln, Germany, Oct. 6-7, 1976.

23. ASTM E 24.03.03, "Proposed Standard Method of Tests for Instrumented Impact Testing of Precracked Charpy Specimens of Metallic Materials", Draft 2c, American Society for Testing and Materials, Philadelphia, U.S.A. 1980.

24. Böhme, W., and Kalthoff, J.F., "The Behavior of Notched Bend Specimens in Impact Testing", Intl. J. Fracture, Vol. 20, 1982, pp. R139-143.

25. Kalthoff, J.F., Winkler, S., Böhme, W. and Klemm, W., "Determination of the Dynamic Fracture Toughness K_{Id} in Impact Tests by Means of Response Curves", 5th Intl. Conf. Fracture, Cannes, March 29 - April 3, 1981, Advances in Fracture Research, Ed. D. Francois et al., Pergamon Press, Oxford, New York, 1980.

26. Ravi Chandar, K., and Knauss, W.G., private communication.

27. Kalthoff, J.F., and Winkler, S., "Fracture Behavior under Impact", Progress Reports prepared for United States Army, European Research Office, London, under Contract No. DAJA 37-81-C-0013, Freiburg, 1983.

28. Kanninen, M.F., Gehlen, P.C., Barnes, C.R., Hoagland, R.G., and Hahn, G.T., "Dynamic Crack Propagation under Impact Loading", Nonlinear and Dynamic Fracture Mechanics, ASME Winter Annual Meeting, New York, Dec. 2-7, 1979, Eds. N. Perrone and S.N. Atluri, ASME-Publication AMD-Vol. 35, 1979.

29. Ahmad, J., Jung, J., Barnes, C.R., and Kanninen, M.F., "Elastic-Plastic Finite Element Analysis of Dynamic Fracture", Engineering Fracture Mechanics, Vol. 17, No. 3, 1983, pp. 235-246

30. Kalthoff, J.F., and Shockey, D.A., "Instability of Cracks under Impulse Loads", J. Appl. Phys., Vol. 48, No. 3, March 1977, pp. 986-993.

31. Shockey, D.A., Kalthoff, J.F., and Ehrlich, D.C., "Evaluation of Dynamic Crack Instability criteria", to appear in Int. J. Fracture,

32. Homma, H., Shockey, D.A., and Muragama, Y., "Response of Cracks in Structural Materials to Short Pulse Loads", submitted to J. Mech. Phys. Solids

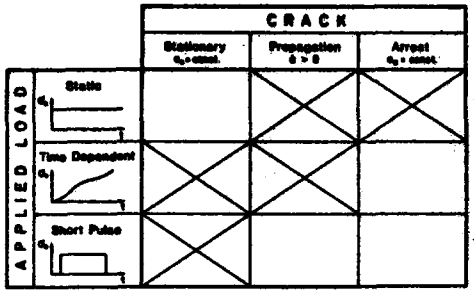

Fig. 1 Dynamic fracture problems

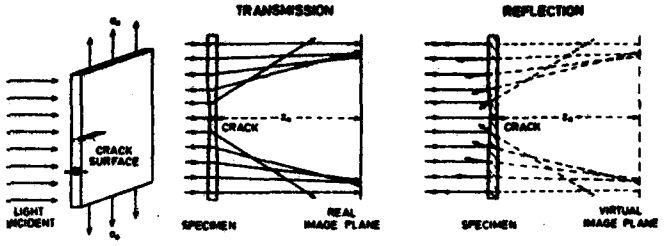

Fig. 2 Shadow optical method of caustics, physical principles

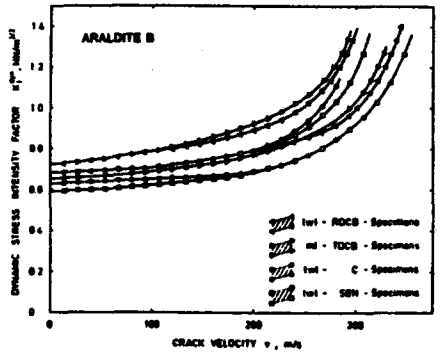

Fig. 4 K-v-data for different test geometries

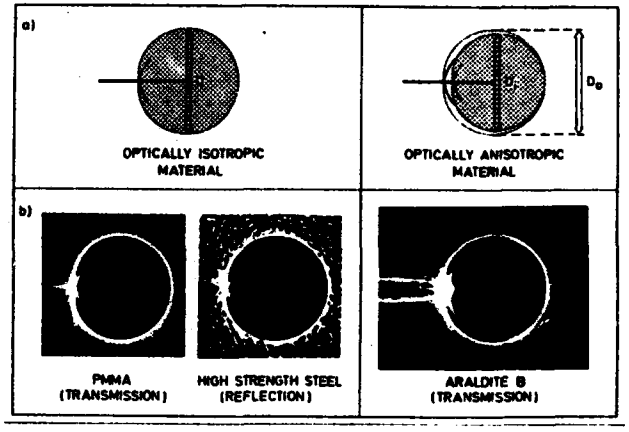

Fig. 3 Caustics

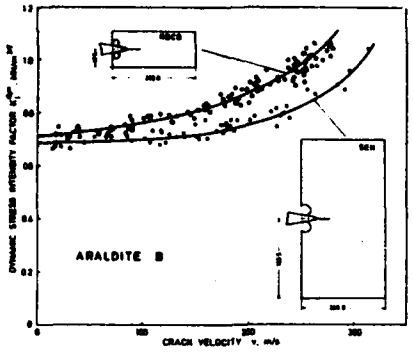

Fig. 5 K-v-data for DCB- and SEN-specimens

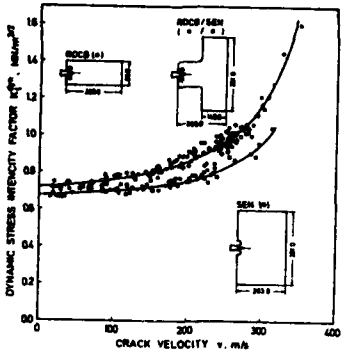

Fig. 6 K-v-data for DCB/SEN-combination specimen

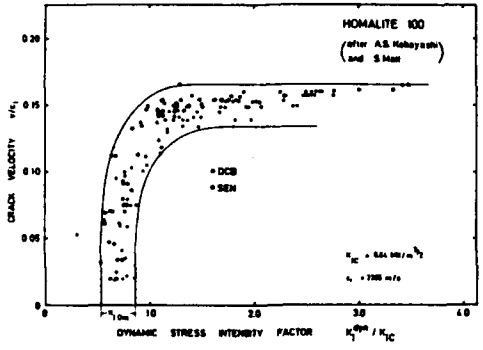

Fig. 7 K-v-data

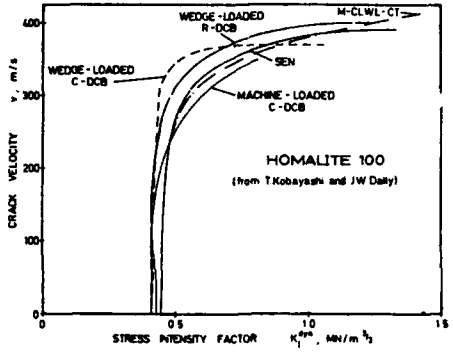

Fig. 8 K-v-data

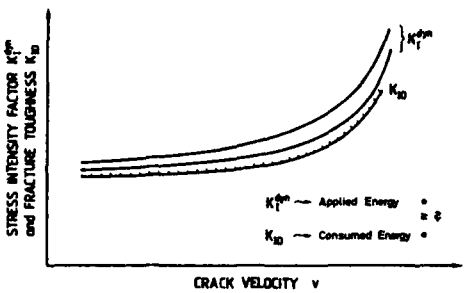

Fig. 9 Dynamic stress intensity factor and fracture toughness

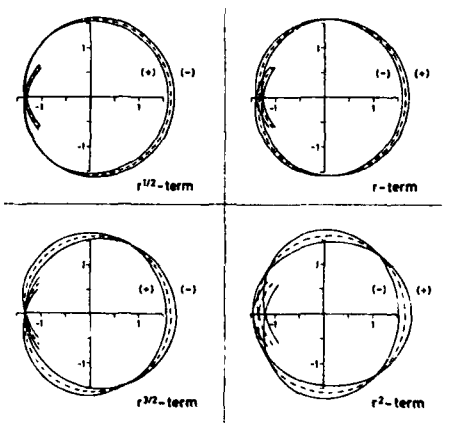

Fig. 12 Influence of higher order terms on caustics

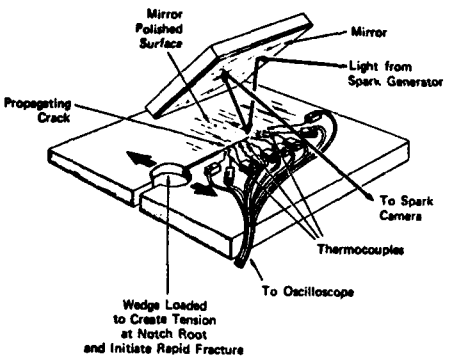

Fig. 10 Simultaneous measurement of K_I^{dyn} and K_{ID}

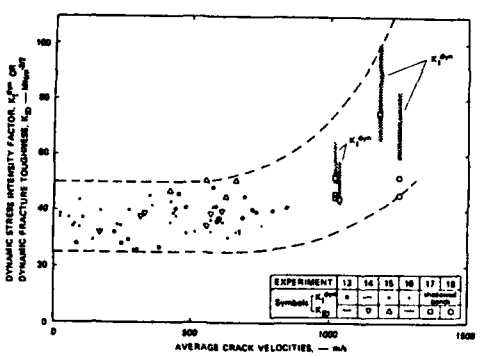

Fig. 11 Measured K_I^{dyn}- and K_{ID}-values

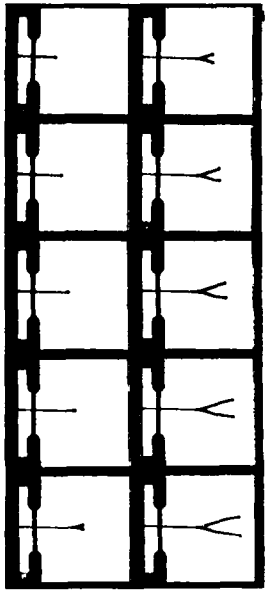

Fig. 13 Crack branching

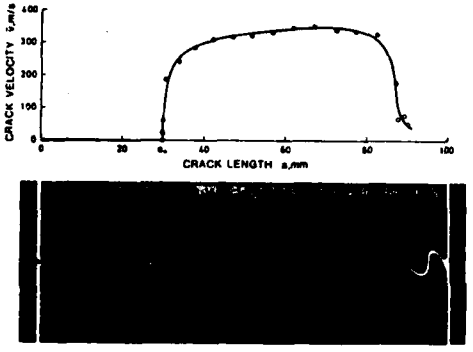

Fig. 14 Fracture behavior of impacted bend specimens

Fig. 16 Mixed mode caustic in impacted bend specimen

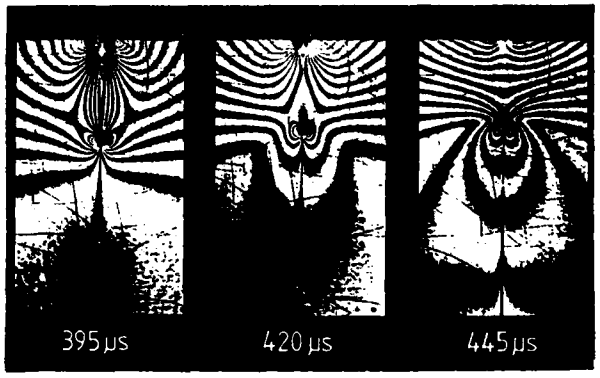

Fig. 15 Photoelastic investigation of crack propagation in impacted bend specimen

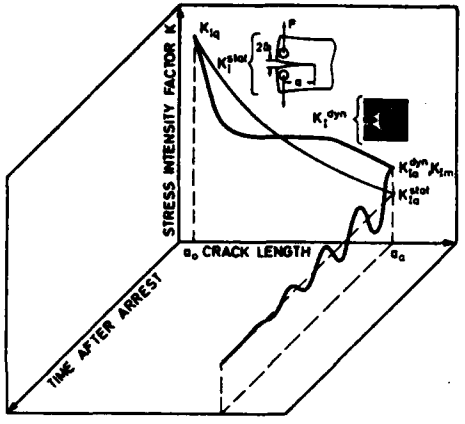

Fig. 17 Crack arrest behavior

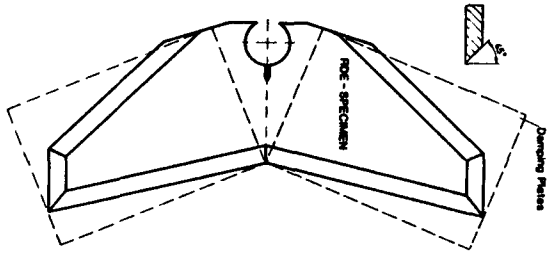

Fig. 19 RDE-crack arrest specimen

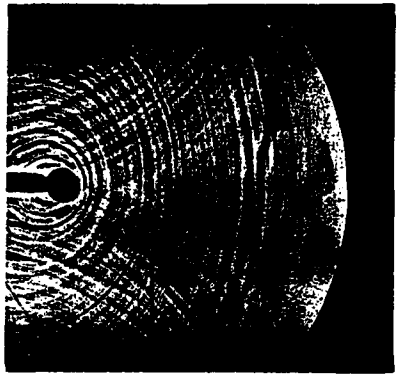

Fig. 18 Shadow optical photograph of a propagating crack in steel

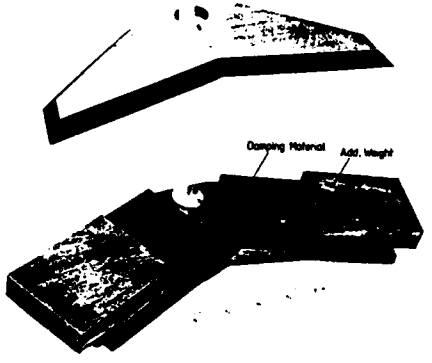

Fig. 20 Photograph of RDE-crack arrest specimen

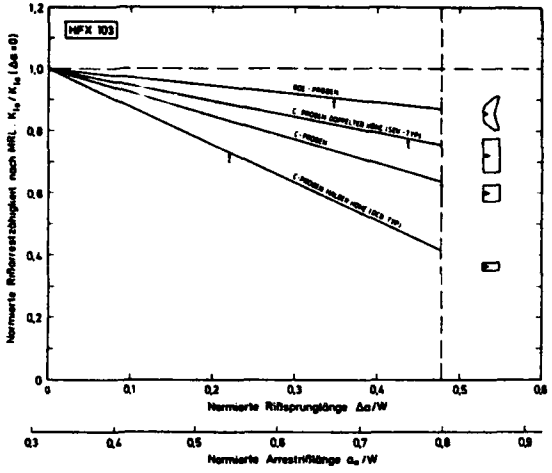

Fig. 21 Dynamic effects for different crack arrest specimens

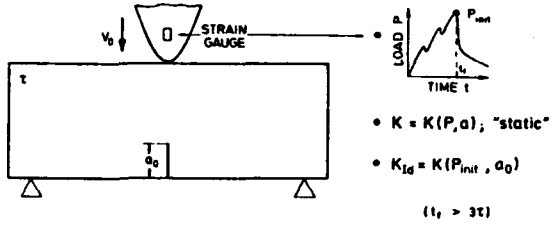

Fig. 22 Determination of the impact fracture toughness

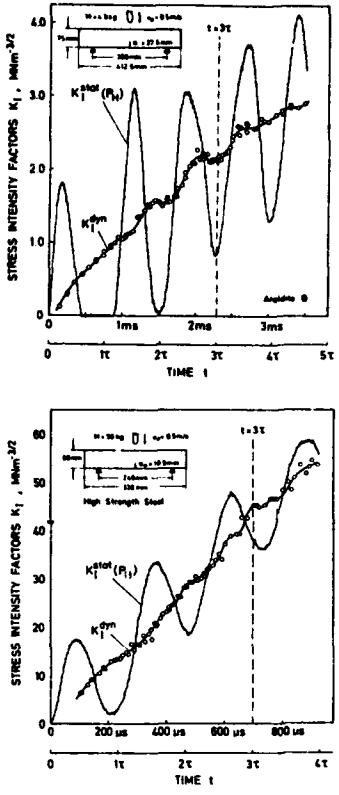

Fig. 23 Stress intensity factors for impacted cracks

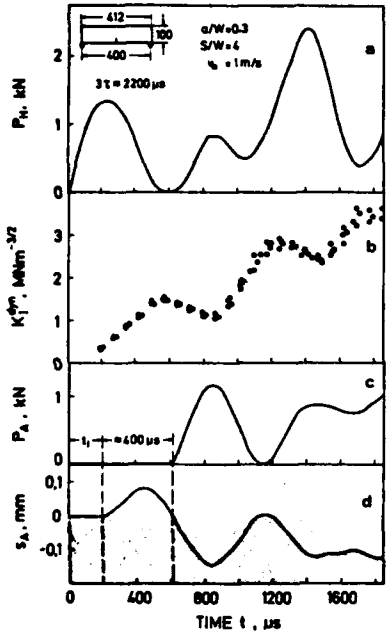

Fig. 24 Specimen behavior under impact loading

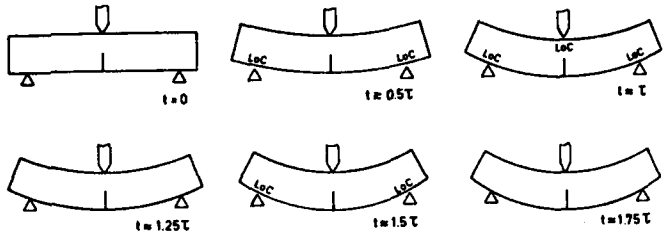

Fig. 25 Loss of contact effects

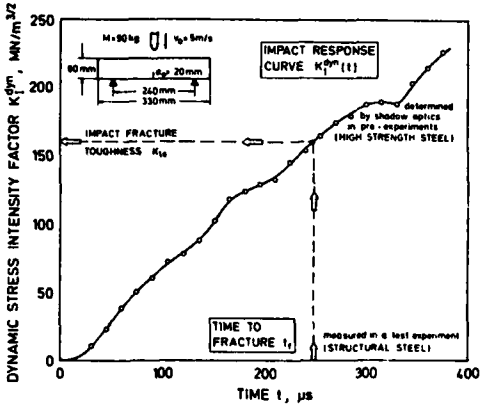

Fig. 26 K_{Id}-determination by impact response curves

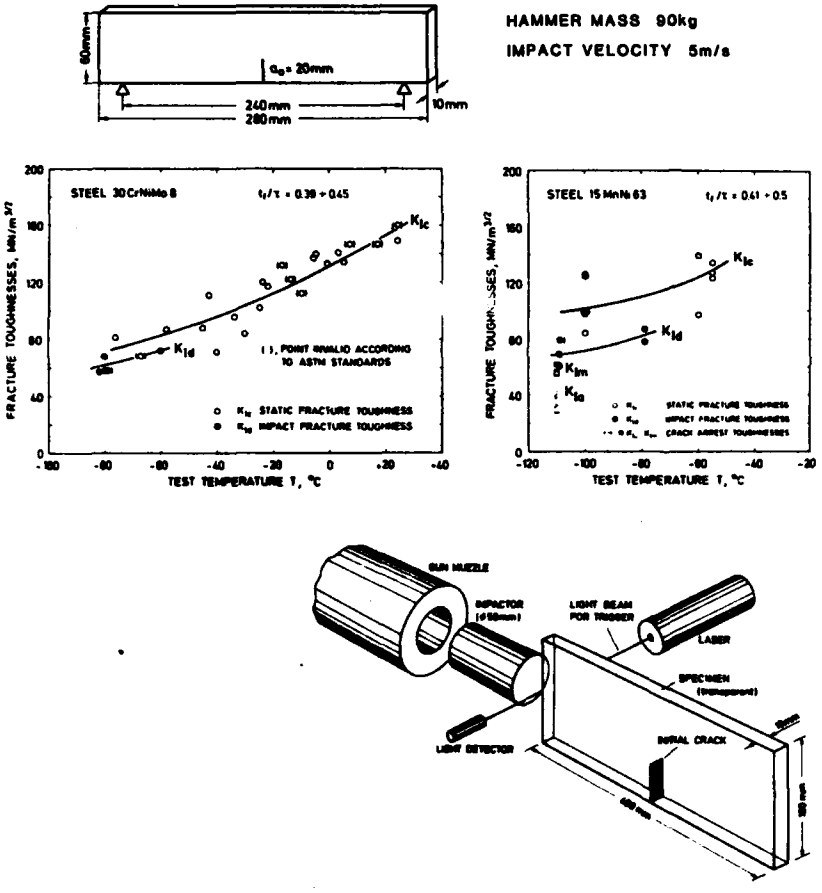

Fig. 27 Impact fracture toughness data

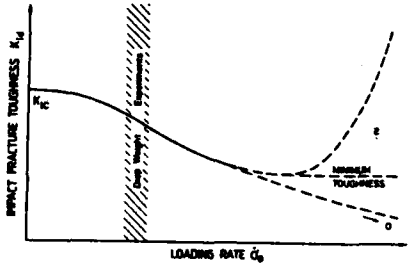

Fig. 28 Influence of loading rate

Fig. 29 Projectile loading arrangement

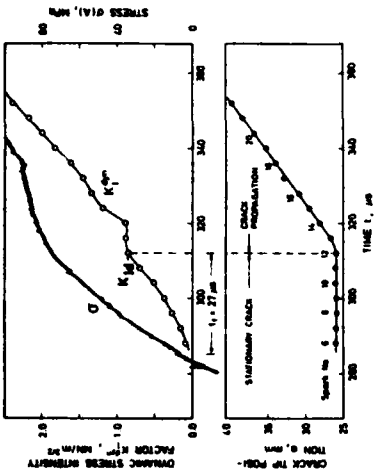

Fig. 31 Fracture behavior under impact loading

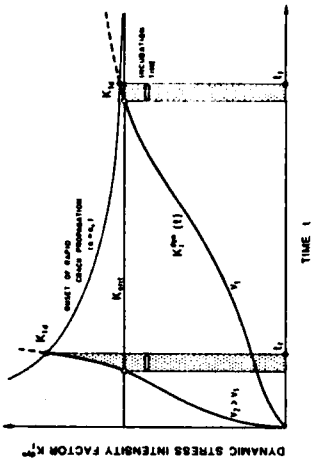

Fig. 33 Incubation time

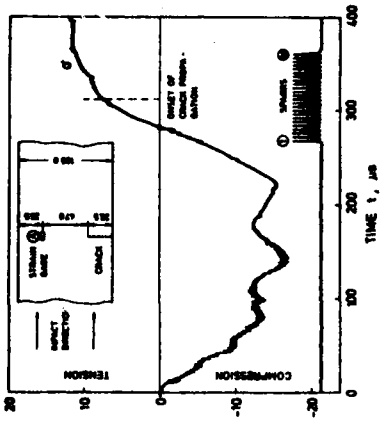

Fig. 30 Load history

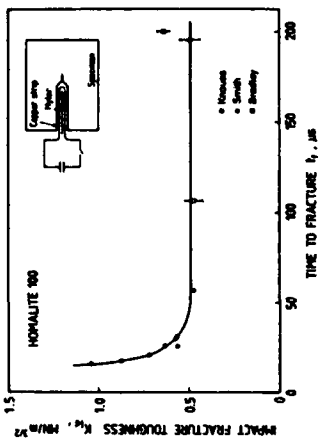

Fig. 32 Loading rate influence

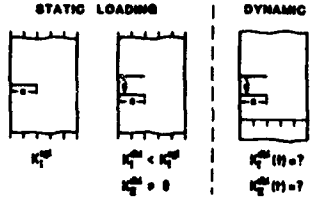

Fig. 34 Interaction of cracks

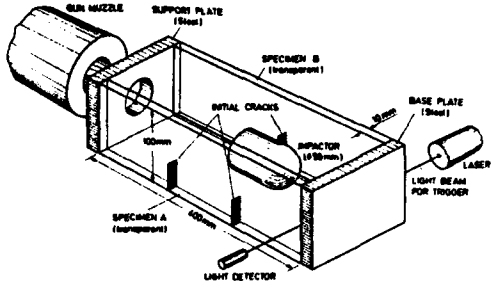

Fig. 35 Loading arrangement

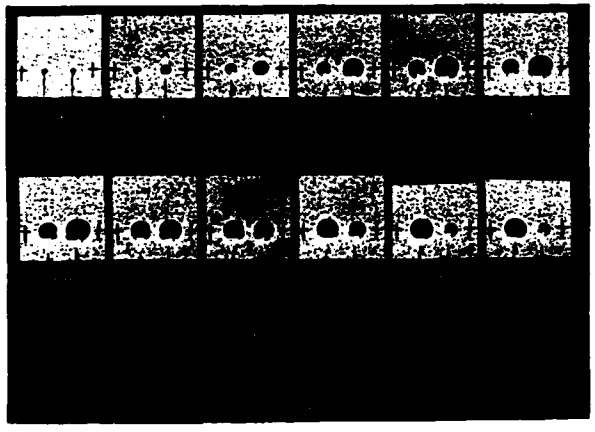

Fig. 36 Dynamic interaction of cracks

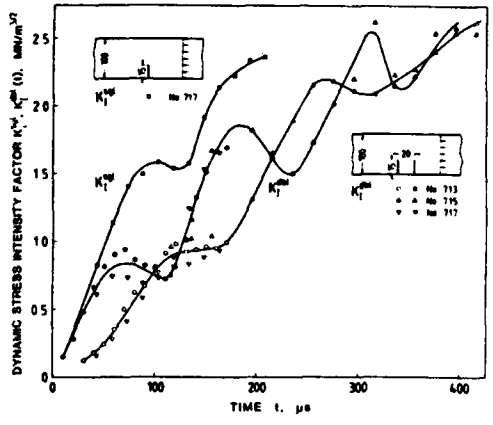

Fig. 37 Stress intensity factors for interacting of cracks

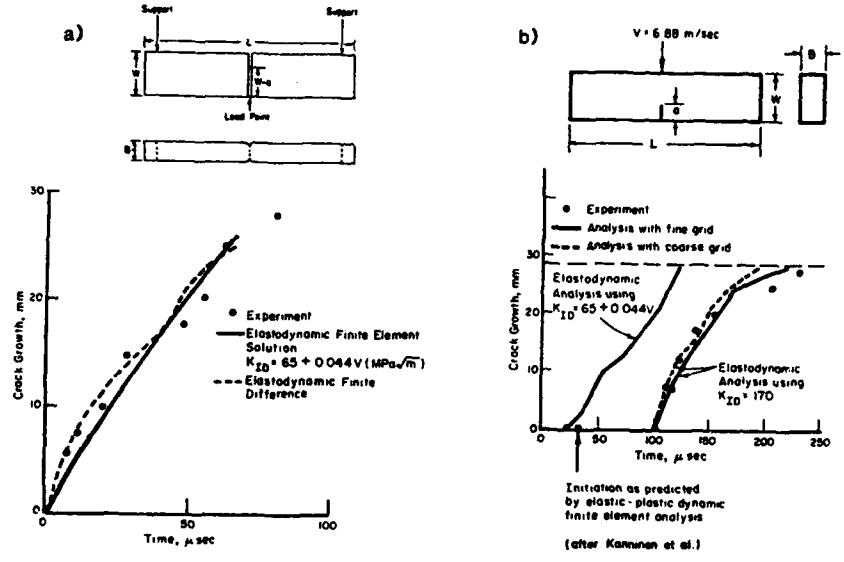

Fig. 38 Crack growth in 4340 steel under a) quasistatic and b) impact loading (after Kanninen et al. [28,29])

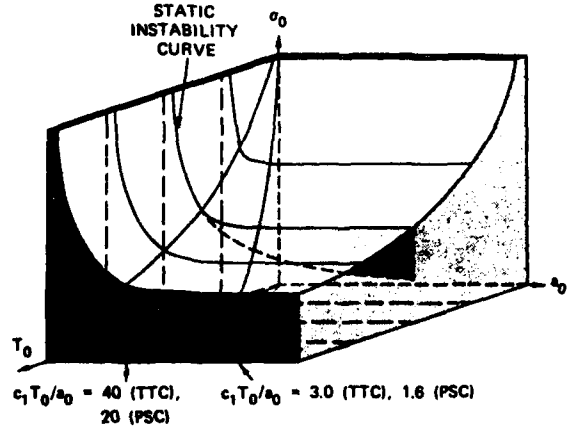

Fig. 39 Dynamic instability surface

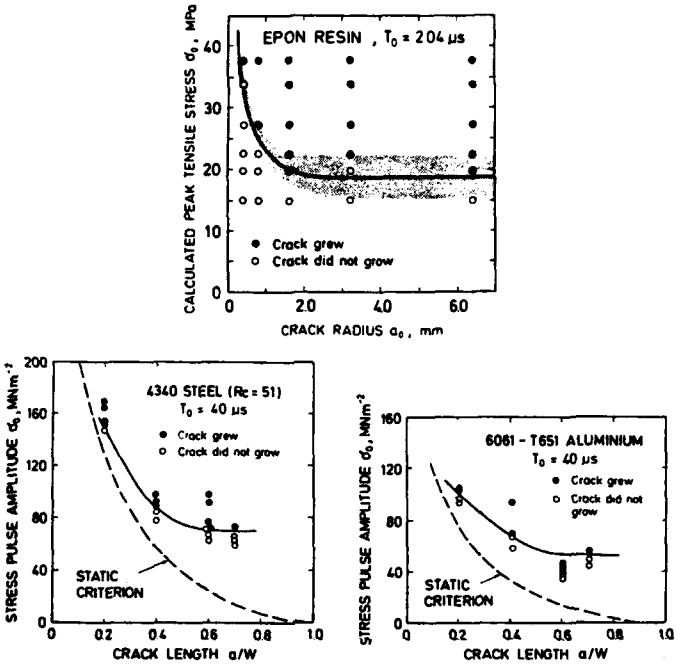

Fig. 40 Dynamic instability data

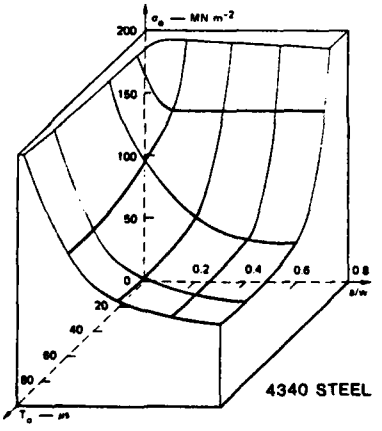

Fig. 41 Measured dynamic instability surface

INTERNATIONAL CONFERENCE

CZECHOSLOVAKIA

June 1983 - Valtice

DYNAMICAL MECHANICAL PROPERTIES AND FRACTURE DYNAMICS OF ENGINEERING MATERIALS

Czechoslovak Academy of Sciences

Institute of Physical Metallurgy

Brno - Czechoslovakia

MECHANICAL RESPONSE OF CRACKS TO IMPACT LOADING

J.F. Kalthoff, S. Winkler, W. Böhme
Fraunhofer-Institut für Werkstoffmechanik (IWM)
Wöhlerstr. 11, 7800 Freiburg, West-Germany
and
D.A. Shockey
SRI-International
333 Ravenswood Avenue, Menlo Park, California, 94025, U.S.A.

1. INTRODUCTION

The concept of fracture mechanics has successfully been applied for describing fracture processes under static loading conditions. Very often static fracture mechanics approaches are also utilized for analyzing dynamic fracture phenomena. This paper discusses the mechanical response of cracks under impact loading. Precracked bend specimens under drop weight loading and cracks under short pulse loading are considered (see Fig. 1). The limitations of static evaluation procedures are shown and fully dynamic concepts are outlined which accurately describe the observed dynamic behavior under all test conditions.

2. DROP WEIGHT LOADING OF PRECRACKED BEND SPECIMENS

A procedure [1] has been proposed to ASTM for measuring the impact fracture toughness K_{Id} of steels with precracked Charpy specimens in instrumented impact tests. The procedure assumes that dynamic stress intensity factors can be determined from loads registered at the tup of the striking hammer via static stress intensity factor formulas, if the times of interest are larger than three times the period τ of the eigenoscillation of the specimen (see Fig. 2).

2.1. Dynamic Effects

The applicability of this approach has been checked by comparing statically determined stress intensity factors, denoted K_I^{stat}, with the actual dynamic stress intensity factors, K_I^{dyn} [2]. The dynamical values have been de-

termined by means of the shadow optical method of caustics and high speed photography. For details of the shadow optical technique see [3,4]. The experiments were performed with specimens of enlarged size made from the model material Araldite B and a high strength steel, tested under drop weight loading at 0.5 m/s. Fig. 3 gives a schematic view of the experimental set-up showing the shadow optical arrangement in reflection with a high strength steel specimen. The results are shown in Fig. 4. The times are given in absolute units and also in relative units by normalization with the period τ. Marked differences were measured between K_I^{stat} und K_I^{dyn}, even for times $t > 3\tau$. Due to different contact stiffnesses, the dynamic effects are more pronounced with Araldite B specimens than with high strength steel specimens. Furthermore, it was found that fracture times $t_f > 3\tau$ could only be obtained by utilizing low impact velocities [2].

The behavior of specimens under impact loading was further investigated by also measuring the specimen reaction at the anvils [5]. Fig. 5 compares the load measured at the striking hammer (a), the stress intensity factor measured at the crack tip (b), the load measured at the anvils (c), and the position of the specimen ends with regard to the anvils (d). The data were obtained with Araldite B specimens impacted at 1 m/s. The τ-value of these specimens is about 700 μs. Non zero loads at the anvils were registered only after a rather long time of about 600 μs. This behavior is explained by diagram (d), Fig. 5. A loss of contact is observed between the specimen ends and the anvils directly after impact. Only at later times ($t \approx 600\ \mu s$) the specimen ends come into contact with the anvils, and in accordance with this observation load values are then recorded at the anvils. With different test conditions this loss of contact can later occur for a second time and loss of contact can also take place between the hammer and the specimen (see Fig. 6). Since in the reported experiments the anvils obviously were of no influence during the early phase of the impact process, additional experiments have been performed with unsupported specimens. The results are represented by the dashed curve and open data points in Fig. 5. In accordance with speculation, the early specimen reaction ($t \leq \tau$) is the same for both, the supported and the unsupported specimen. The measured behavior demonstrates the strong influence of inertial effects during impact loading. It is concluded, therefore, that the determination of reliable impact fracture toughness values K_{Id} at reasonably high loading rates does require a fully dynamic evaluation procedure.

2.2. The Concept of Impact Response Curves

At IWM the dynamic concept of impact response curves has been developed for determining impact fracture toughness data (see Fig. 7 and [6]): For fixed test conditions (i.e. specimen geometry, hammer mass, impact velocity, etc.) the dynamic stress intensity factor versus time relationship is determined by means of the shadow optical method of caustics with an edge notched high strength steel specimen (see also Fig. 3). The obtained K_I^{dyn}-t-curve, called impact response curve, is controlled by the elastic properties of the system only. It therefore applies for all steels provided the conditions for small scale yielding are fulfilled. In the real test-experiment with precracked specimens of the steel to be investigated, then only the time to fracture is measured (e.g. by an uncalibrated strain gage near the crack tip). This time together with the preestablished impact response curve determines the impact fracture toughness value K_{Id} (see Fig. 7).

Impact response curves are shown in Fig. 8. The curves were obtained with specimens of different sizes and different ratios of specimen length to support span. The specimens were impacted by a hammer of 90 kg or 260 kg at a velocity of 5 m/s. Specimens which were supported at the very ends of the specimen show a more oscillatory K_I^{dyn}-t-curve. Specimens with a length to support span ratio L/S = 55/40 (as with Charpy specimens) are characterized by a more steadily increasing curve (see also [5]).

Impact fracture toughness values K_{Id} determined from these response curves are shown in Fig. 9 for the steels 30 CrNiMo 8 and 15 MnNi 63 and in Fig. 10 for a pressure vessel steel. Some of the K_{Id}-values are compared with static fracture toughness data. Although crack instability occurred at relatively small loading times ($t_f < \bar{\tau}$) the concept of impact response curves gave reliable data.

2.3. One Point Bend Experiment

In the experiments reported above the specimens failed at very early times and consequently the anvils did not influence the specimen reaction (see 2.1). Since at higher loading rates the specimens would fail even earlier, it is natural that a high rate impact test (> 5 m/s) for measuring K_{Id}-values

can be based on a "one point bend" experiment, utilizing unsupported specimens (see Fig. 11a).

The impact response curve for an unsupported steel specimen is shown in Fig. 11b. The specimen was 270 mm long and 50 mm wide, the crack length was 15 mm. Impact loading was achieved by a projectile of 1.92 kg mass which was accelerared by a gas gun to a velocity of 17 m/s. The stress intensity factor capacity of the loading arrangement is about 260 $MN/m^{3/2}$. Fracture toughness measurements have been performed with specimens made from a mild steel. Specimens of 20 mm thickness were tested at $-10^{o}C$, $+20^{o}C$, and $+50^{o}C$. The loading conditions were the same as before. Complete failure of the specimens was observed in all experiments. Fig. 12 shows the fracture surfaces of the broken specimens, the times to fracture t_f, and the dynamic fracture toughness values K_{Id}. These preliminary data demonstrate the feasibility of the one point bend technique for measuring impact fracture toughness data, in particular at high loading rates.

Additional experiments have been performed at a lower impact velocity of 5 m/s with a pendulum type of impact tester. The test device was slightly modified to load unsupported specimens of size 280 x 60 x 10 mm^3. The hammer mass was 20 kg. Mild steel specimens were tested at $-50^{o}C$, $-10^{o}C$, and $+20^{o}C$. The results are shown in Fig. 13. The room temperature specimen was only partly broken, but at the lower temperatures complete failure of the specimens was obtained inspite of the only modest impact velocity.

Further work will be performed at IWM to study the practical applicability of the one point bend test.

3. SHORT PULSE LOADING OF CRACKS

At SRI-International Shockey et al. and Kalthoff [7-9] studied the fracture behavior of cracks loaded by stress pulses of durations which are comparable or even smaller than the time it takes waves to travel the distance given by the crack length. Data of short pulse experiments are reported and a dynamic instability criterion is presented which describes the experimental findings.

3.1. Experimental Instability Data

According to the static fracture mechanics concept critical stresses for instability should continuously decrease with increasing crack length, as shown schematically in Fig. 14. Shockey et al. [7,8] measured the instability stresses for cracks of different lengths which were subjected to stress pulses of different durations. The stress pulses were produced by plate impact or projectile impact techniques. For experimental details see [7,8]. Results obtained with specimens made from an epoxy resin and 4340 steel are summarized in Figs. 15 and 16. The data indicate the following behavior: For short cracks the instability stresses decrease with increasing crack length, similar as in static fracture mechanics. For cracks above a certain length, however, higher stresses are needed to bring a crack to instability than under static loading conditions. Furthermore, the instability stresses seem not to depend on crack length but to be constant.

3.2. Short Pulse Fracture Criterion

For cracks which are loaded by stress pulses of short duration a simple $\sigma_0\sqrt{\pi \cdot a_0}$-relationship does not apply anymore. Instead the behavior is controlled by a rather complex stress intensity history [9]. Dynamic stress intensity factors for cracks subjected to step function loads were calculated by Sih et al. [10]: The stress intensification first increases with time according to a square root of time relationship, overshoots the equivalent static stress intensity factor by a considerable amount, and then reaches a constant static value after damped oscillations. Based on these results the stress intensity histories were derived for cracks of increasing length subjected to a rectangular stress pulse of duration T_0 (see Fig. 17, [9]). For convenience the crack length a_0 in Fig. 17 is measured in units $c_1 \cdot T_0$; c_1 is the longitudinal wave speed. For short cracks ($a_0 < \frac{1}{24} c_1 T_0$) the stress intensity history is characterized by an almost rectangular shape and the average stress intensity factor is identical with the equivalent static stress intensity factor value. With increasing crack length the stress intensification becomes larger and more triangular in shape, but the average dynamic stress intensity is smaller than the stress intensity factor value

for the equivalent static crack. For even larger crack lengths ($a_0 > \frac{1}{3} c_1 T_0$) the dynamic stress intensification does not increase anymore but stays the same although the crack length and accordingly the static stress intensity factor increases.

Assuming that the crack has to experience a supercritical stress intensity factor for at least a certain minimum time in order to become unstable, a short pulse fracture criterion was developed [9]. According to this criterion and the stress intensity history discussed above, higher critical stresses are predicted to bring a crack above a certain length to instability than in the equivalent static case. Furthermore, the predicted instability stresses do not depend on crack length. The general instability behavior of cracks with different lengths subjected to different loading conditions, i.e. pulse amplitudes and pulse durations, is shown in a three-dimensional (σ_0-a_0-T_0)-diagram, see Fig. 18. The short pulse fracture behavior is represented in the rear right section of the diagram, the front left regime (long pulse durations, short crack lengths) shows the usual static behavior.

The experimental data (Figs. 14 and 15) represent two-dimensional slices taken through the derived instability diagram for fixed durations T_0. The good agreement between the experimental observations and the theoretical predictions demonstrates the validity of the developed short pulse fracture criterion. The criterion shows the limitations of static fracture mechanics approaches and represents an appropriate tool for describing the fracture behavior of cracks under short pulse loading.

4. SUMMARY

Results on the behavior of notched bend specimens under drop weight loading and of cracks under short pulse loading have been reported. The experimental findings demonstrate the strong influence of dynamic effects. Thus, static evaluation procedures can lead to erroneous results, and are applicable only with restrictions. Reliable dynamic material strength values can only be derived from measured test data on the basis of fully dynamic analyses. The concept of impact response curves and the short pulse fracture criterion have been presented. These fully dynamic approaches are applicable under all

possible test conditions. The determination of impact fracture toughness data at higher loading rates by one point bend experiments is outlined.

REFERENCES

1. ASTM E 24.03.03, "Proposed Standard Method of Tests for Instrumented Impact Testing of Precracked Charpy Specimens of Metallic Materials", Draft 2c, American Society for Testing and Materials, Philadelphia, U.S.A., 1980

2. Kalthoff, J.F., Böhme, W., Winkler, S., and Klemm, W., "Measurements of Dynamic Stress Intensity Factors in Impacted Bend Specimens", CSNI Specialists Meeting on Instrumented Precracked Charpy Testing, EPRI, Palo Alto, Calif., U.S.A, Dec. 1980

3. Beinert, J. and Kalthoff, J.F., "Experimental Determination of Dynamic Stress Intensity Factors by Shadow Patterns" in Mechanics of Fracture, Vol. 7, Ed. G.C. Sih, Martinus Nijhoff Publishers, The Hague, Boston, London, 1981, pp. 281-330

4. Kalthoff, J.F., "Stress Intensity Factor Determination by Caustics", Intl. Conf. Experimental Mechanics, Society for Experimental Stress Analysis and Japan Society of Mechanical Engineers, Honolulu, Maui, Hawaii, U.S.A, May 23-28, 1982

5. Böhme, W., and Kalthoff, J.F., "The Behavior of Notched Bend Specimens in Impact Testing", Intl. J. Fracture, Vol. 20, 1982, pp. R139-143

6. Kalthoff, J.F., Winkler, S., Böhme, W. and Klemm, W., "Determination of the Dynamic Fracture Toughness K_{Id} in Impact Tests by Means of Response Curves", 5th Intl. Conf. Fracture, Cannes, March 29 - April 3, 1981, Advances in Fracture Research, Ed. D. Francois et al., Pergamon Press, Oxford, New York, 1980

7. Shockey, D.A., Kalthoff, J.F., and Ehrlich, D.C., "Evaluation of Dynamic Crack Instability Criteria", to appear in Intl. J. Fracture

8. Homma, H., Shockey, D.A., and Muragama, Y., "Response of Cracks in Structural Materials to Short Pulse Loads", submittet to J. Mech. Phys. Solids

9. Kalthoff, J.F., and Shockey, D.A., "Instability of Cracks under Impulse Loads", J. Appl. Phys., Vol. 48, No. 3, March 1977, pp. 986-993

10. Sih, G.C., Embley, G.T., and Ravera, R.J., "Impact Response of a Plane Crack in Extension", Intl. J. Solids Structures, Vol. 8, 1982, pp. 977-993

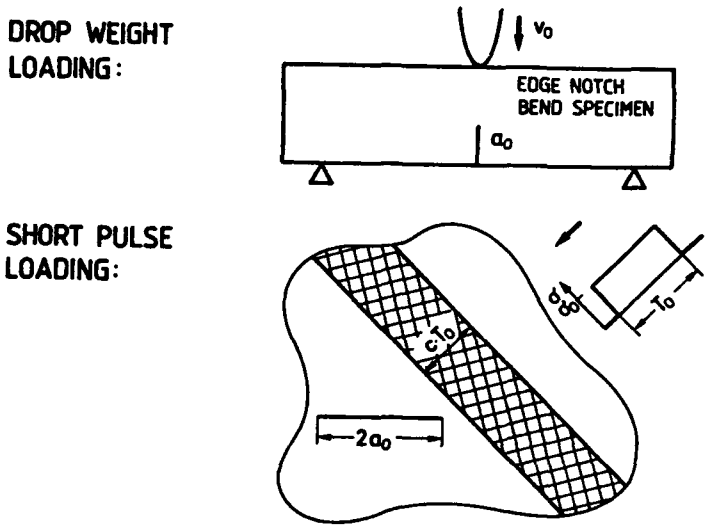

Fig. 1 Impact fracture problems

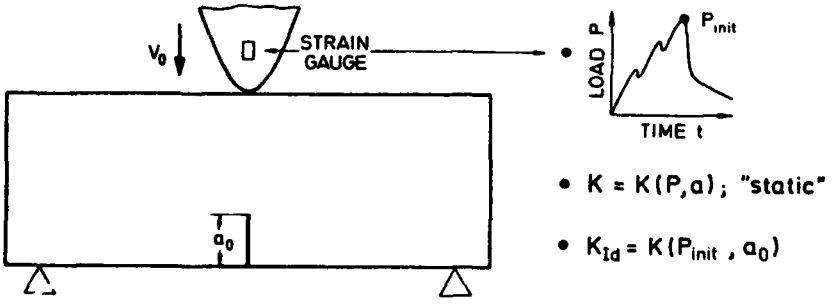

Fig. 2 Determination of the impact fracture toughness K_{Id} in instrumented impact tests

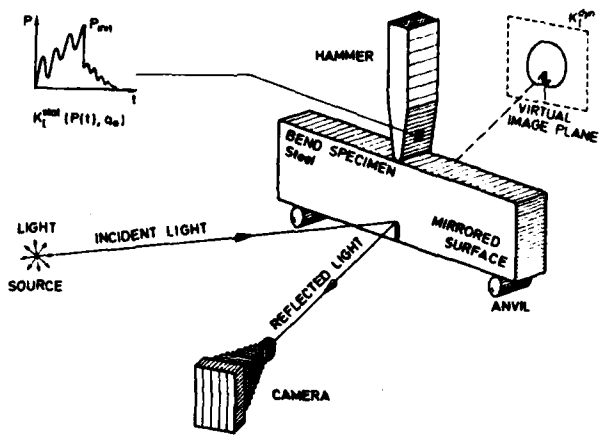

Fig. 3 Experimental set-up showing the shadow optical arrangement in reflection with a high strength steel specimen

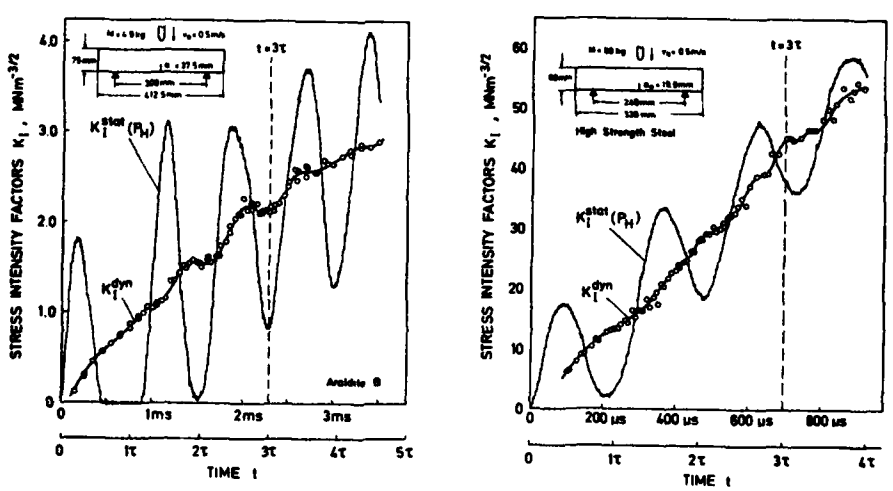

Fig. 4 Stress intensity factors for prenotched bend specimens under drop weight loading

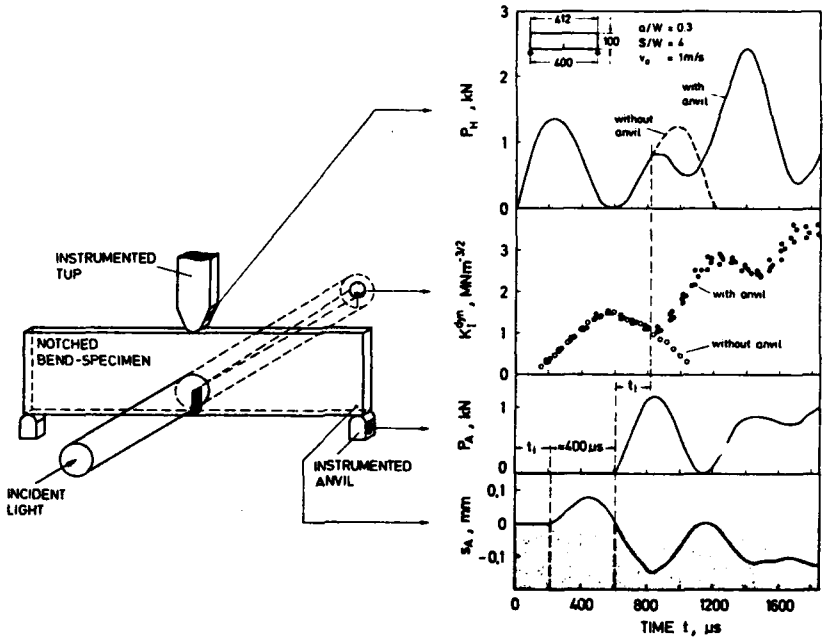

Fig. 5 Mechanical response of prenotched bend specimens to drop weight loading

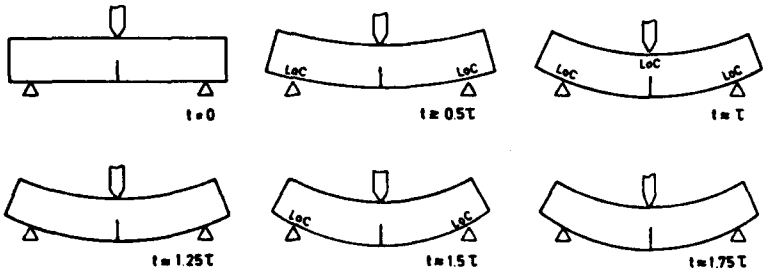

Fig. 6 Loss of contact effects observed with prenotched bend specimens under impact loading

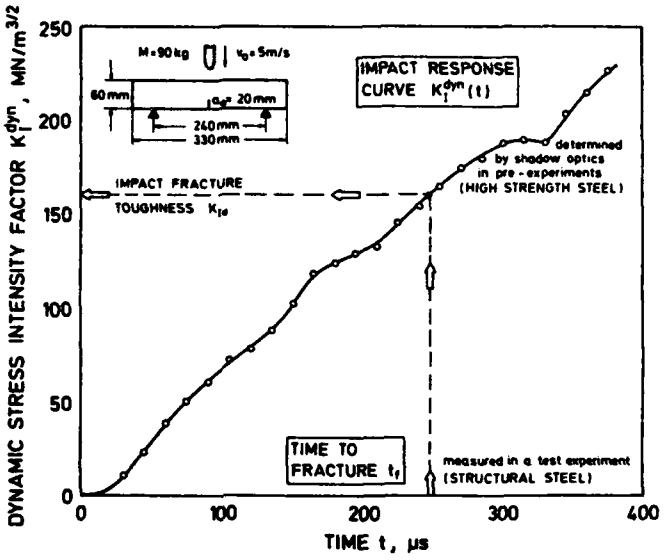

Fig. 7 The concept of impact response curves for measuring the impact fracture toughness K_{Id}

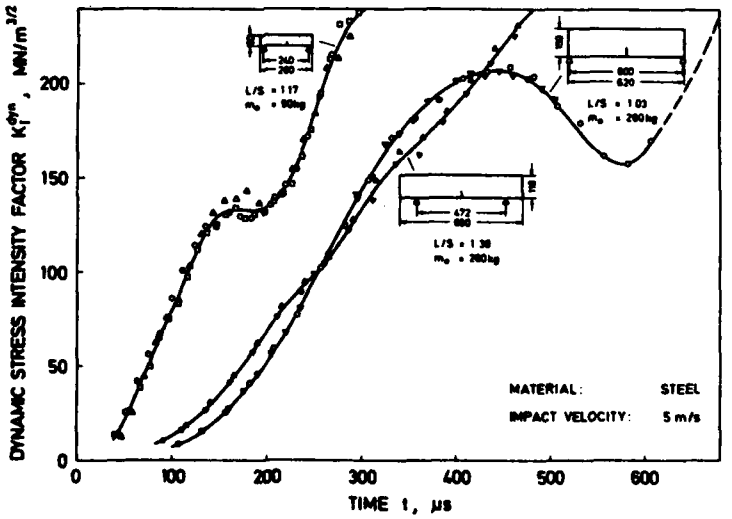

Fig. 8 Impact response curves for different bend specimens

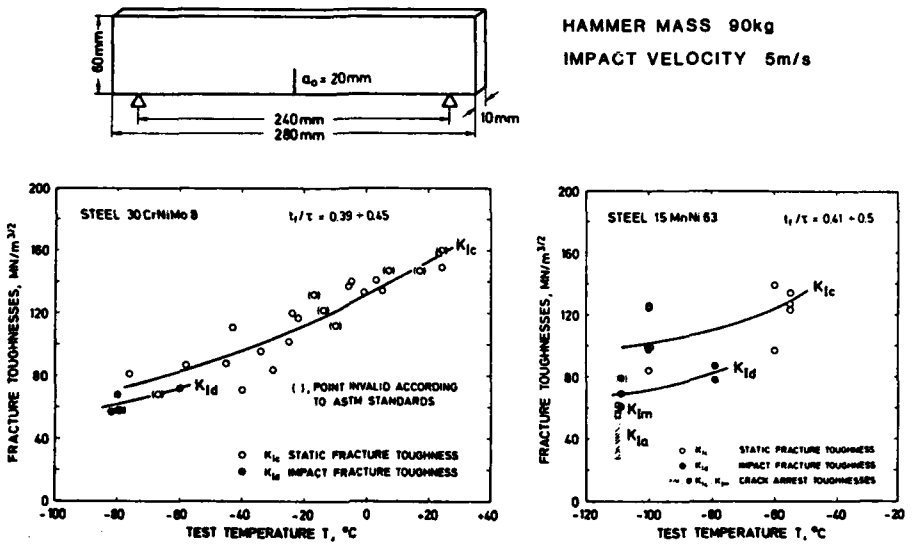

Fig. 9 Impact fracture toughness data

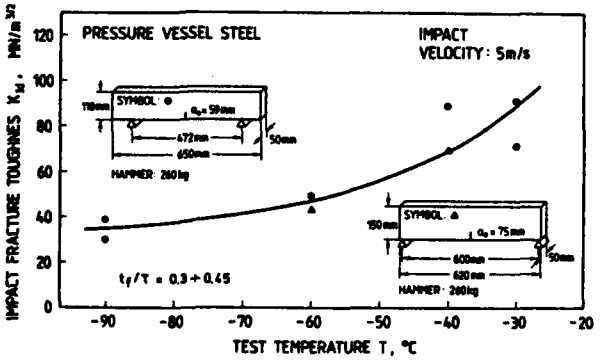

Fig. 10 Impact fracture toughness data

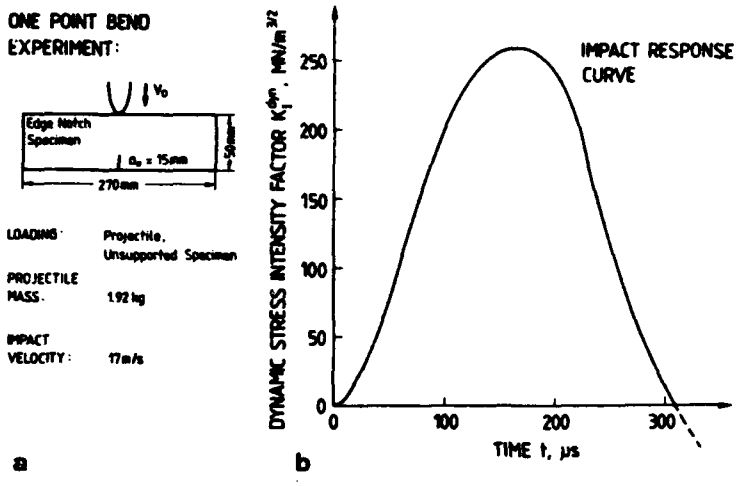

Fig. 11 One point bend technique and impact response curve for an unsupported specimen

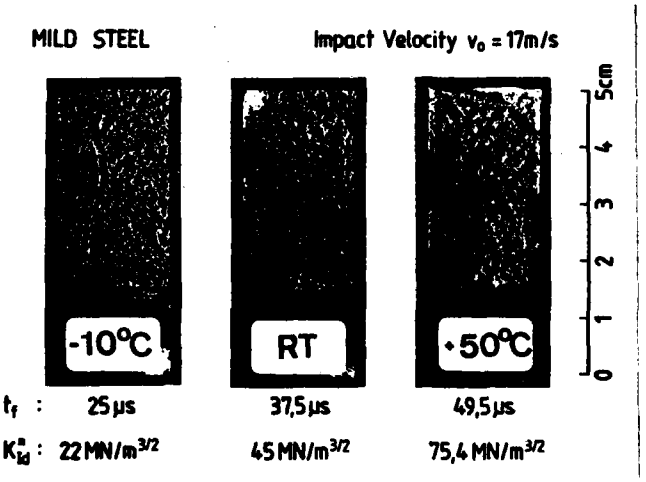

Fig. 12 Fracture data obtained in one point bend experiments

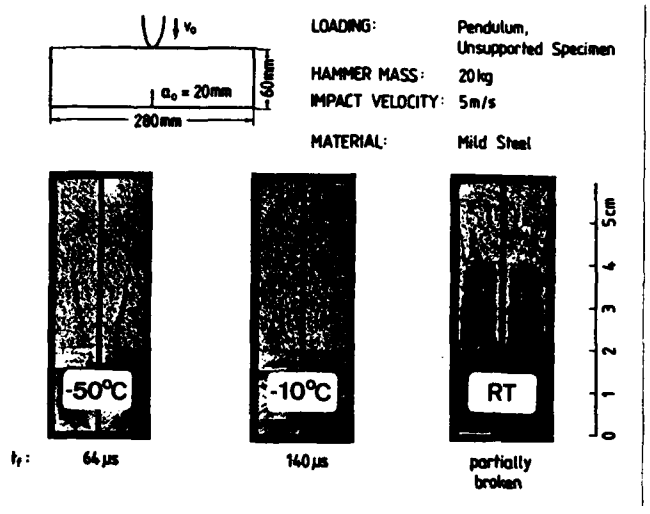

Fig. 13 Fracture surfaces of specimens loaded by the one point bend technique in a modified pendulum impact tester (RT-specimen: heat tinted after impact testing)

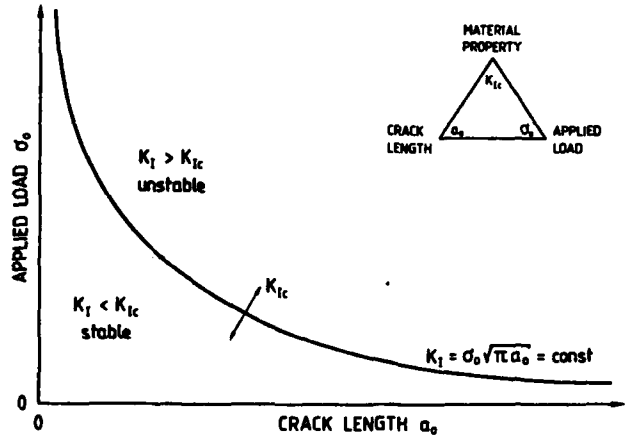

Fig. 14 Instability behavior of cracks under static loading conditions

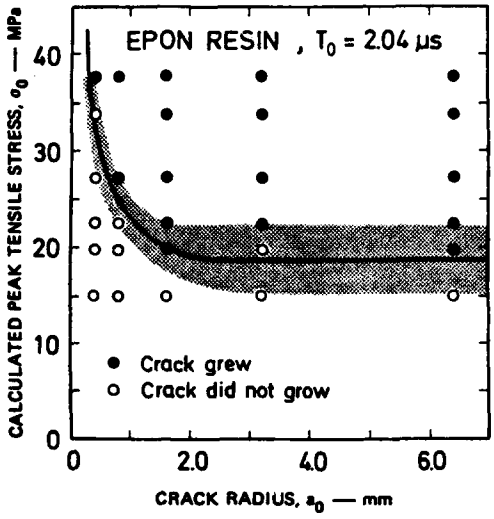

Fig. 15 Instability stresses for cracks under short pulse loading

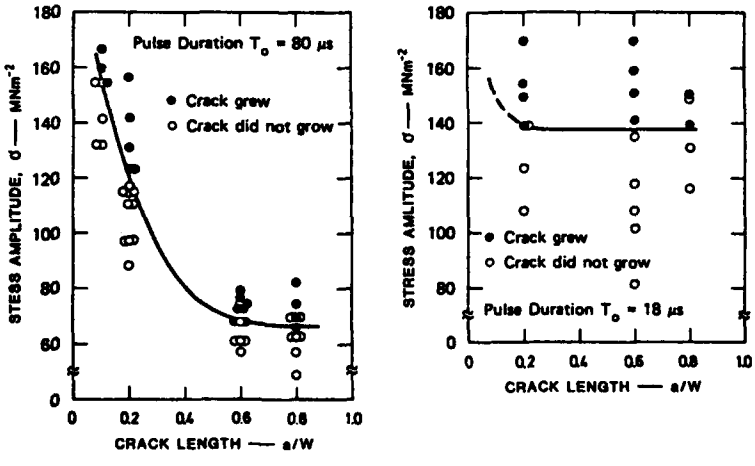

Fig. 16 Instability stresses for cracks under short pulse loading

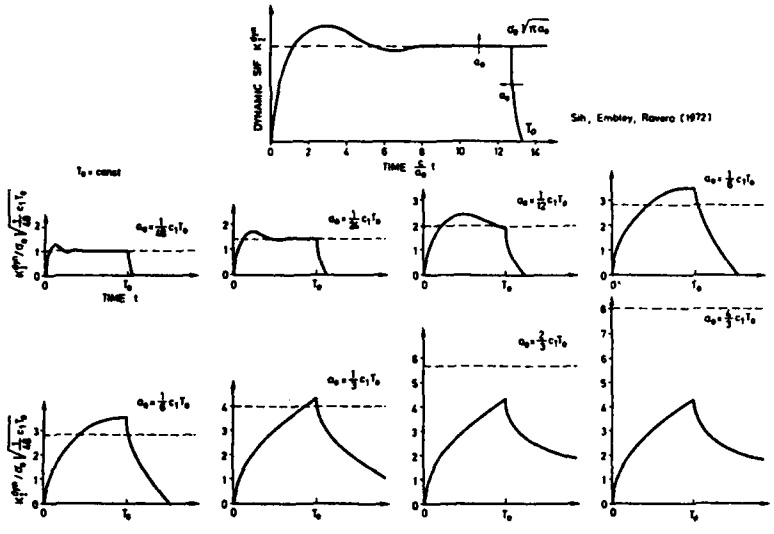

Fig. 17 Stress intensity histories for cracks under short pulse loading

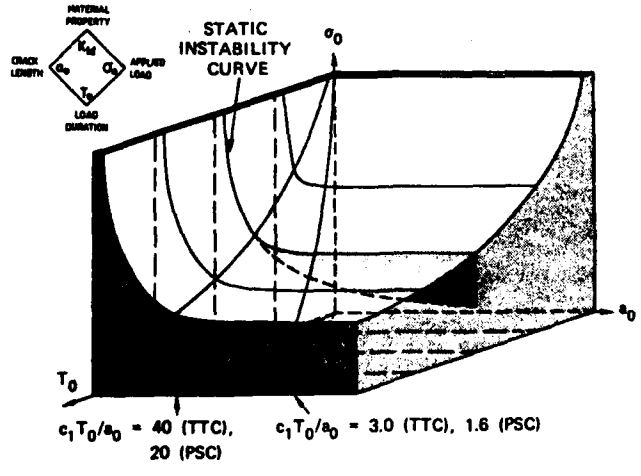

Fig. 18 Dynamic instability surface for cracks under short pulse loading

INTERNATIONAL CONFERENCE ON

AFMMS

APPLICATION OF FRACTURE MECHANICS TO MATERIALS AND STRUCTURES

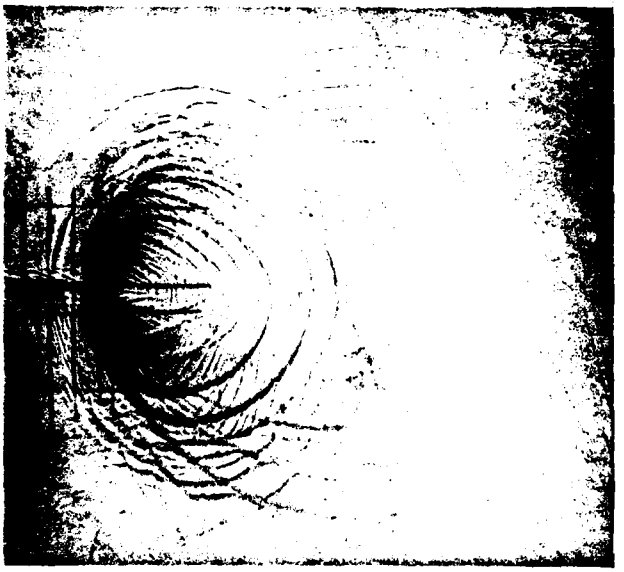

FREIBURG, GERMANY
June 20–24, 1983

Fraunhofer-Institut für Werkstoffmechanik
Wöhlerstraße 11
D-7800 Freiburg, West Germany

TIME EFFECTS AND THEIR INFLUENCES ON TEST PROCEDURES FOR MEASURING DYNAMIC MATERIAL STRENGTH VALUES

J.F. Kalthoff

Fraunhofer-Institut für Werkstoffmechanik, IWM
Wöhlerstr. 11, 7800 Freiburg i.Br., W.-Germany

INTRODUCTION

The strength or the toughness of a material cannot be measured directly. Instead mechanical quantities, i.e. lengths, stresses, stress intensity factors are measured under specific conditions, for example at the beginning of yield, at the onset of rapid fracture, etc. These mechanical quantities in general are also not measured directly, but electronic signals from strain gages as parts of different measuring devices are recorded.

Thus the process of measuring material strength data actually resembles a chain with different links. This is illustrated in Figure 1. The measuring chain starts with the material behavior to be investigated, then the mechanical and electronic aspects follow, and it ends with the established material value. This is illustrated by a simple example in Figure 1: the ductility of a material is to be measured, and it shall be characterized by the yield stress. Then the mechanical aspect of the measuring problem is defined by the fact that stresses are obtained by dividing the applied force by the cross sectional area. Furthermore, if the force is measured by a strain gage, the electronic aspect of the problem consists of gage calibration, i.e. in establishing a relation of the form: force = calibration factor x change in electric voltage. Thus the quantity "stress" is traced back to secondary quantities and the specific value of the derived term at yield then finally represents the yield stress. This example is trivial and problems along this measuring chain do not usually occur when static material strength data are determined. The situation, however, is very different when dynamic material data shall be measured. Influences of time on the material behavior are to be measured, but time effects can also have an influence on the mechanical and electronic aspects of the measuring procedure. In fact, these latter effects can be even larger than the effect on the material itself. Since the material value shall only reflect the influences of time effects on the material behavior but not on the mechanical and the electronic aspects, erroneous data can result if the mechanical analysis or the electronic system are not appro-

priate for the problem considered. Procedures for measuring reliable dynamic material strength values, therefore, require and have to be based upon

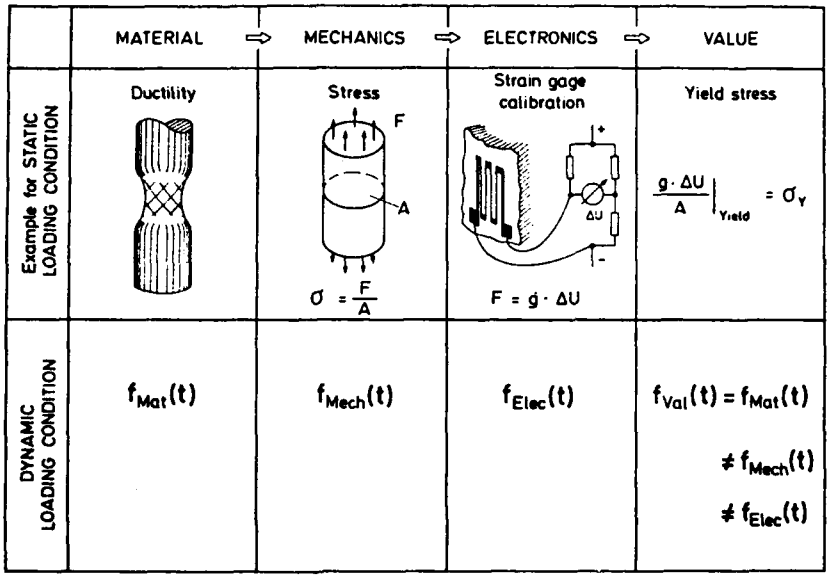

Fig. (1) - Basic principle of procedures for measuring material strength values

a complete knowledge and understanding of the mechanical and electronic aspects of the measuring procedure.

This paper considers the mechanical aspects and gives an example of the electronic aspects associated with the determination of dynamic fracture toughness values, in particular of the crack arrest toughness and of the initiation fracture toughness at high loading rates.

MECHANICAL ASPECTS

In this chapter the mechanical behavior of propagating and subsequently arresting cracks, of cracks under impact loading by a pendulum or a drop weight, and of cracks under short pulse loading is discussed. An illustrative view of the problems considered is given in Figure 2. The dynamic influences are demonstrated by comparing the actual dynamic reactions at the crack tip with the equivalent static behavior. Most of the dynamic

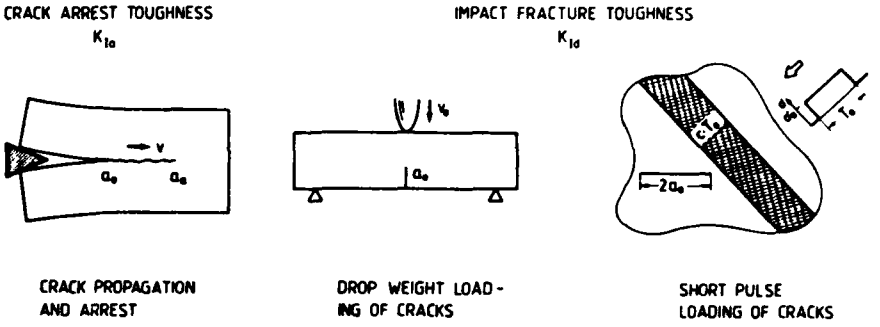

Fig. (2) - Dynamic fracture problems

data reported have been determined by means of the shadow optical method of caustics. This technique is briefly described first, the fracture data are presented in the following sections.

A. The Shadow Optical Method of Caustics

The method of caustics is an optical tool for measuring stress intensifications. The technique has been introduced by Manogg in 1964 [1,2]. Later on, Theocaris [3] further developed the method. The author and his coworkers extended and applied Manoggs technique for investigating dynamic fracture phenomena [4-6].

The physical principle of the method is illustrated in Figure 3. A precracked specimen under load is illuminated by a parallel light beam. A cross-section through the specimen at the crack tip is shown in Figure 3b

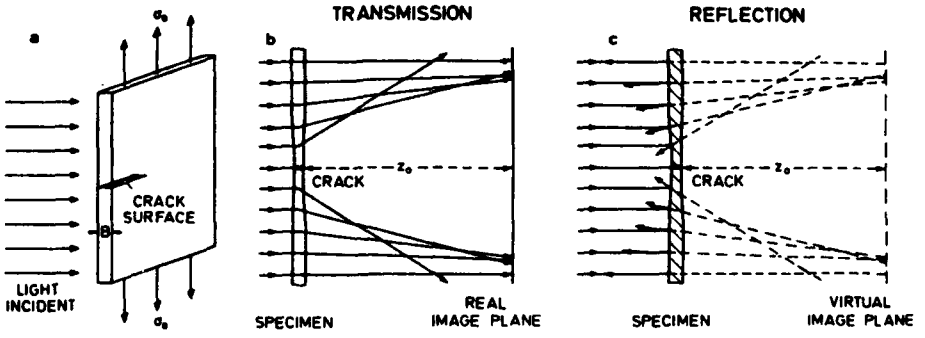

Fig. (3) - Physical principle of the shadow optical method of caustics

for a transparent specimen, and in Figure 3c for a non-transparent steel specimen. Due to the stress concentration the physical conditions at the crack tip are changed. For transparent specimens both the thickness of the

specimen and the refractive index of the material are reduced. Thus, the area surrounding the crack tip acts as a divergent lens and the light rays are deflected outwards. As a consequence, on a screen (image plane) at a distance z_o behind the specimen a shadow area is observed which is surrounded by a region of light concentration, the caustic (see Figure 4). Figure 3c shows the situation for a non-transparent steel specimen with a mirrored front surface. Due to the surface deformations light rays near the crack tip are reflected towards the center line. An extension of the reflected light rays onto a virtual image plane at the distance z_o behind the specimen results in a light configuration which is similar to the one obtained in transmission. Consequently a similar caustic is obtained. The mode I shadow pattern was calculated by Manogg [1] from the linear elastic stress strain field around the crack tip. Figure 4 compares theoretical results with experimentally observed caustics which were photographed

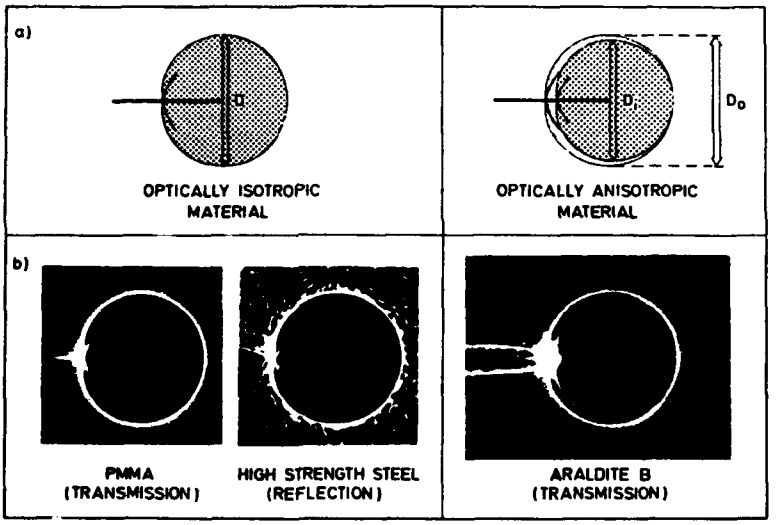

Fig. (4) - Mode I caustics, a) calculated, b) measured

in transmission and in reflection with different materials. The single caustic curve obtained for isotropic materials splits up into a double caustic for optically anisotropic materials.

The size of the shadow pattern is related to the stress intensification at the crack tip. The quantitative correlation between the diameter D of the caustic and the stress intensity factor K_I is given by the relation

$$K_I = \frac{2\sqrt{2\pi} \cdot F(v)}{3 f_{o,i}^{5/2} \cdot c \cdot d_{eff} \cdot z_o} D^{5/2} \qquad (1)$$

where K_I = Mode I stress intensity factor,
D = diameter of the caustic,
$f_{o,i}$ = numerical factor for outer/inner caustic,
c = photoelastic constant,
d_{eff} = effective thickness of the plate,
= d for transparent specimens,
= d/2 for reflecting, non-transparent specimens,
d = physical thickness of the plate,
z_o = distance between specimen and image plane,
$F(v)$ = correction factor for non-zero crack velocities, $F(v) \lesssim 1$,
v = crack velocity.

Numerical values of the constants which appear in the K-evaluation formula are given in Table 1 for different materials. For further details of the shadow optical technique see [4-6].

TABLE (1) - CONSTANTS FOR CAUSTIC EVALUATION

	Elastic Constants		Shadow Optical Constants						Effective Thickness
			for Plane Stress			for Plane Strain			
Material	Young's Modulus MN/m²	Poisson's Ratio	c m²/N	f_o	f_i	c m²/N	f_o	f_i	d_{eff}
TRANSMISSION ($z_o < 0$)									
Optically Anisotropic									
Araldite B	3680*	0.392*	-0.970×10^{-10}	3.31	3.05	-0.580×10^{-10}	3.41	2.99	d
CR-39	2586	0.443	-1.200×10^{-10}	3.25	3.10	-0.560×10^{-10}	3.33	3.04	d
Plate Glass	73900	0.231	-0.027×10^{-10}	3.43	2.98	-0.017×10^{-10}	3.62	2.97	d
Homalite 100	4820*	0.310*	-0.920×10^{-10}	3.23	3.11	-0.767×10^{-10}	3.24	3.10	d
Optically Isotropic									
PMMA	3240	0.350	-1.080×10^{-10}	3.17		-0.750×10^{-10}	3.17		d
REFLECTION ($z_o > 0$)									
All materials	E	v	2v/E	3.17		-	-		d/2

Crack tip caustics are of a simple form and can easily be evaluated, the technique, therefore, is very well suited for investigating complex phenomena, as e.g. in fracture dynamics. A Cranz Schardin 24 spark high speed camera is utilized in these investigations for photographing shadow patterns under dynamic loading conditions.

B. Arresting Cracks

The usual procedure for measuring the crack arrest toughness K_{Ia} of a material is the following: In a wedge loaded specimen a fast propagating crack is initiated from a blunted initial notch at an initiation stress intensity factor $K_{Ig} > K_{Ic}$. Figure 5 shows a rectangular double cantilever beam specimen under longitudinal wedge loading. The crack opening displacement remains constant during crack propagation due to the

stiffness of the loading system. Thus the crack propagates into a decreasing stress intensity factor field. It arrests at the lengths a_a if conditions for crack propagation are not fulfilled anymore. This threshold value represents the crack arrest toughness K_{Ia}.

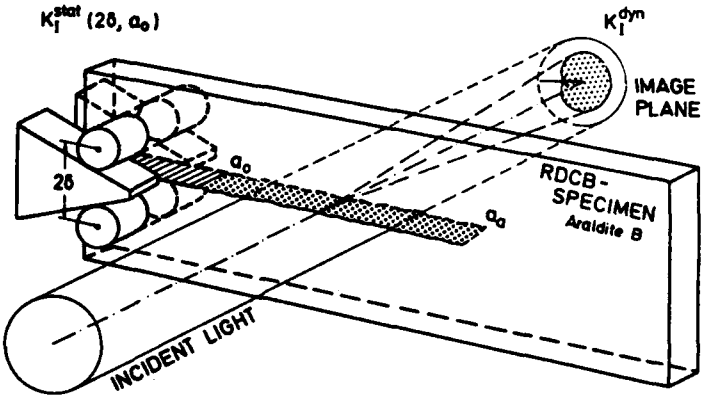

Fig. (5) - Experimental set-up for a crack arrest experiment and shadow optical arrangement in transmission (schematically)

In order to investigate the influences of dynamic effects on the mechanical behavior of cracks at arrest, the stress condition at the tip of a propagating and subsequently arresting crack was analyzed [7-10]. The results of experiments [7,8] with specimens made from a transparent model material, the epoxy resin Araldite B, are reported. The actual dynamic stress intensity factors, K_I^{dyn}, were measured by means of the shadow optical method of caustics in transmission. These values are compared to the equivalent static stress intensity factors, K_I^{stat}, calculated from the measured crack opening displacement 2δ utilizing conventional stress intensity factor formulas.

A series of six shadow optical photographs is shown in Figure 6. Quantitative data for cracks initiated at different K_{Iq}-values are presented in Figure 7. The dynamic stress intensity factors, K_I^{dyn} (experimental points), are shown as a function of crack length together with the corresponding static stress intensity factor curves, $K_I^{stat}(a)$. In addition, the measured crack velocities are given in the lower part of the diagram. The following characteristics of the crack arrest process can be deduced from these results: At the beginning of the crack propagation phase the dynamic stress intensity factor K_I^{dyn} is smaller than the corresponding static value K_I^{stat}. At the end of the propagation phase, in particular at the moment of arrest, the dynamic stress intensity factor K_I^{dyn} is larger than the corresponding static value K_I^{stat}. Only after arrest does the dynamic stress intensity factor K_I^{dyn} approach the static stress intensity factor at arrest, K_{Ia}^{stat}. Differences between the dynamic and the static stress intensity factor curves become smaller for cracks initiated

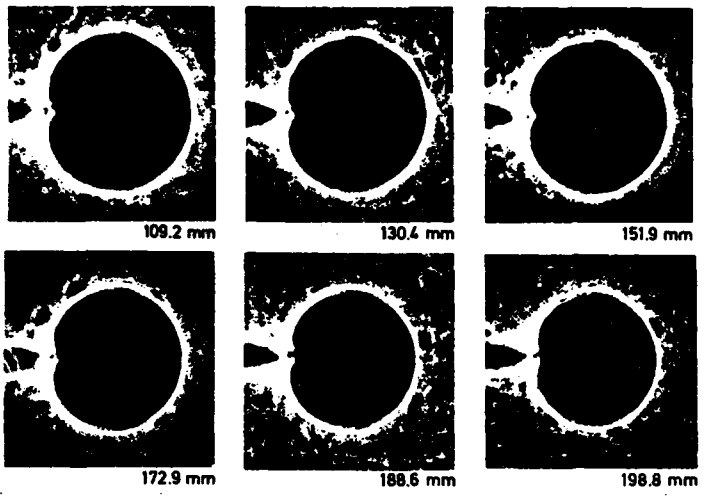

Fig. (6) - Caustics for a propagating and subsequently arresting crack (photographed in transmission with an Araldite B specimen)

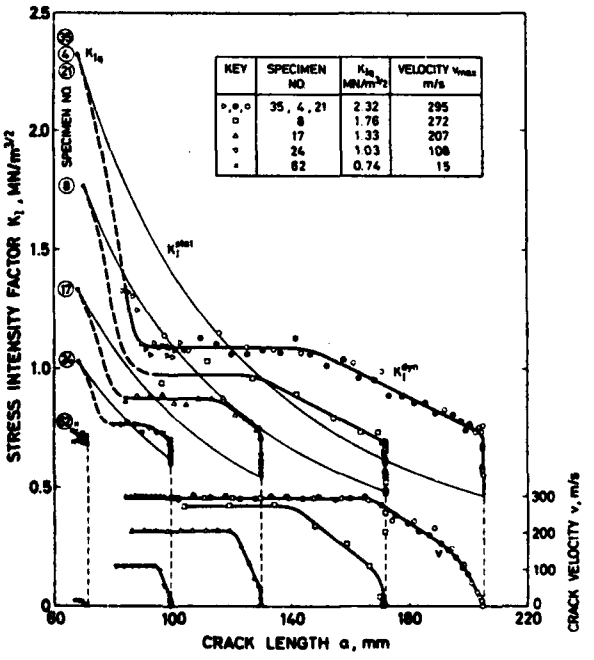

Fig. (7) - Stress intensity factors and crack velocity for propagating and subsequently arresting cracks

at lower K_{Ia} values, i.e. for cracks propagting at lower velocities. The dynamic effects obviously decrease with decreasing velocity, as one might expect.

The behavior of the dynamic stress intensity factor in the post-arrest phase is shown in Figure 8. The dynamic stress intensity factor, K_I^{dyn}, is plotted as a function of time. K_I^{dyn} oscillates around the value of the

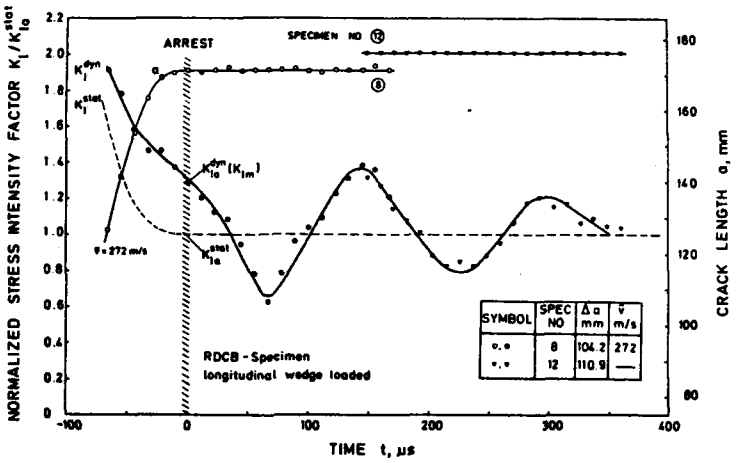

Fig. (8) - Post-arrest behavior

static stress intensity factor at arrest, K_{Ia}^{stat}. Only a large time after arrest the dynamic stress intensity factor approaches the static value. The experimental findings are summarized in the schematic representation of Figure 9.

Wave propagation phenomena explain the observed behavior: elastic waves are produced by the propagating crack, thus kinetic energy is radiated into the specimen and $K_I^{dyn} < K_I^{stat}$. After reflection at the finite boundaries of the specimen the waves then interact with the crack again and contribute to the stress intensity factor, consequently $K_I^{dyn} > K_I^{stat}$. An illustrative view of these processes is given in Figure 10. A fast propagating crack (1000 m/s) in a high strength steel specimen was photographed in a shadow optical reflection arrangement [8]. In addition to the shadow spot at the crack tip the photograph shows the generation of waves at the tip of the propagating crack and the subsequent reflection at the boundaries of the specimen.

Consequently, the stress condition at arrest is not static but dynamic, although the crack velocity is zero at the moment of arrest. Crack arrest toughness values which are determined on the basis of static evaluation procedures [11,12] in principle, therefore, cannot represent a true material property. Statically determined crack arrest toughness values K_{Ia}^{stat} are

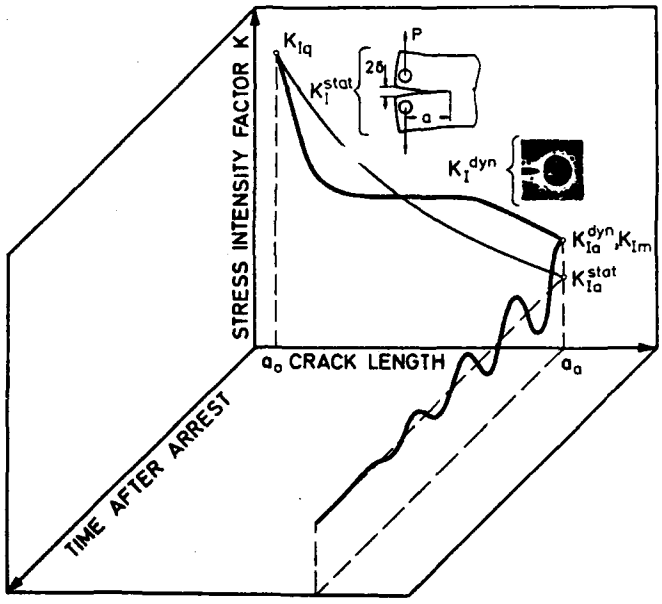

Fig. (9) - Crack arrest behavior (schematically)

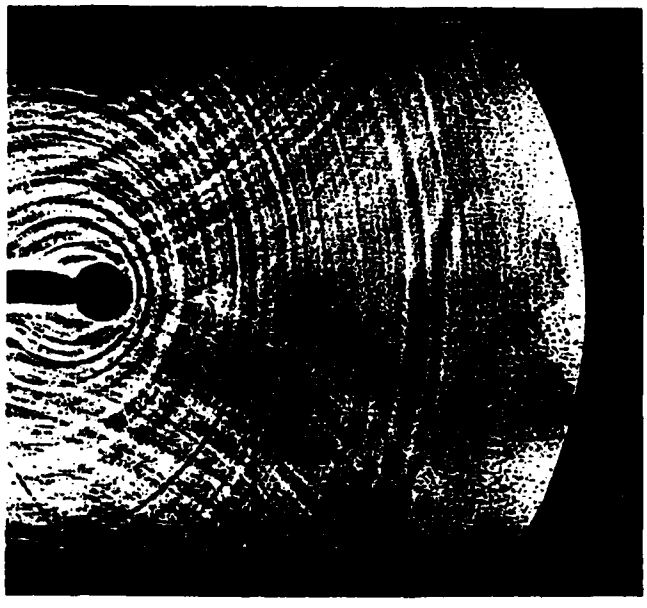

Fig. (10) - Shadow optical photograph of a fast propagating crack in steel

smaller than the true dynamically determined crack arrest tougness values, K_{Ia}^{dyn} (see Figure 9). The determination of the true crack arrest toughness has to take the dynamic effects into account and requires a fully dynamic analysis, for example the Battelle concept of recovered kinetic energy [13,14]. The differences between statically and dynamically determined crack arrest toughness values depend on the shape and size of the specimen [8] and can be quite remarkable, in particular for larger crack jump distances. Figure 11 compares the results of an ASTM cooperative test program obtained with compact crack arrest test specimens (see data in [15]).

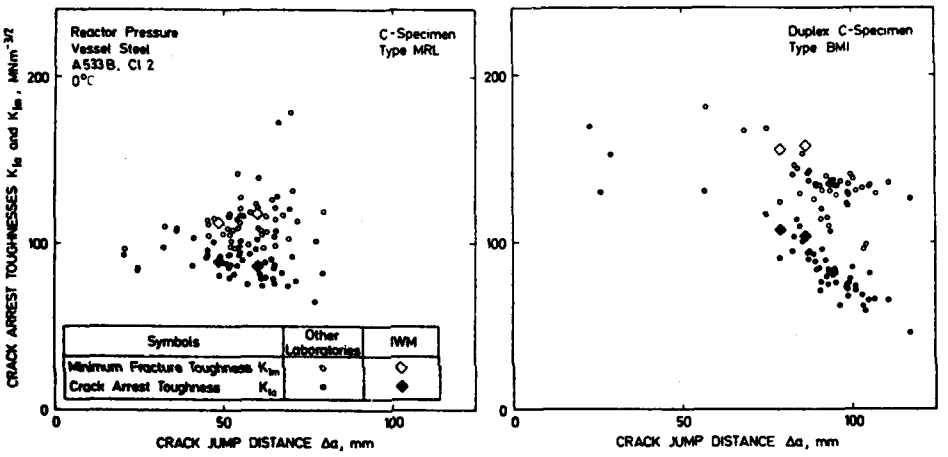

Fig. (11) - Crack arrest toughness data from ASTM Cooperative Test Program, $K_{Ia} \hat{=} K_{Ia}^{stat}$ - determined according to a static analysis [11,12], $K_{Im} \hat{=} K_{Ia}^{dyn}$ - determined according to a fully dynamic analysis [13,14]

Safety predictions on the basis of K_{Ia}^{stat} data therefore can be erroneous. However, since the dynamic effects in large scale structures are in general smaller than in the relatively small laboratory test specimens which are used for K_{Ia} determination, static crack arrest analyses will yield conservative crack arrest predictions [16]. On the basis of this understanding the static crack arrest concept can be applied by the practical engineer under certain circumstances.

In order to minimize the errors in the static crack arrest concept a special crack arrest specimen with reduced dynamic effects has been developed at IWM. This RDE-(reduced-dynamic-effects)-specimen is shown in Figures 12 and 13. The edges and boundary of the specimen are shaped to reduce wave reflections and to defocus reflected waves. Damping material and additional weights are attached to the "wings" of the specimen to absorb kinetic energy and to increase the period of the eigenoscillation of the specimen, thus the recovery of kinetic energy is reduced. Details are

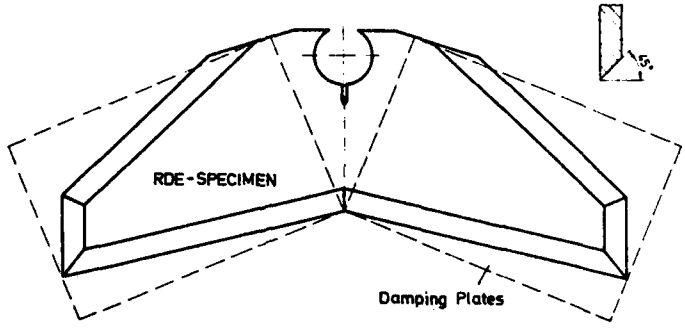

Fig. (12) - RDE-crack arrest test specimen

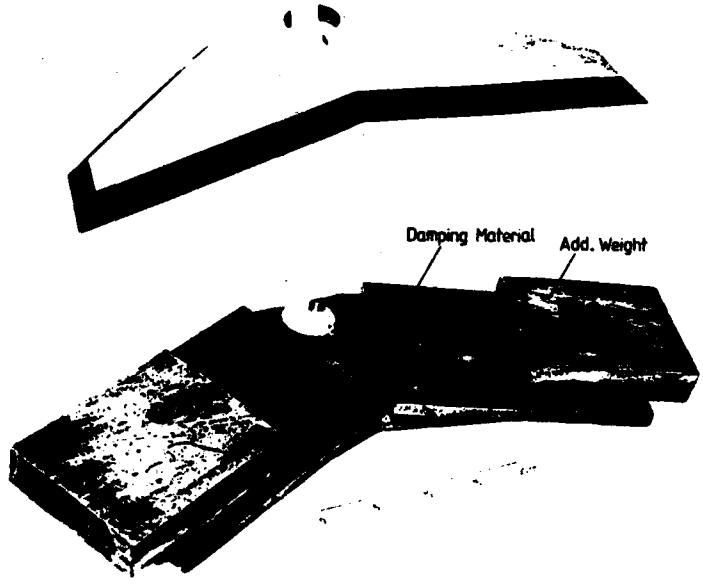

Fig. (13) - Photographs of RDE-crack arrest test specimen

described by Beinert and Kalthoff [17]. Dynamic effects in the RDE-specimen are three to four times smaller than in the most commonly used compact crack arrest specimen. Thus, with specially designed specimens, as for example the RDE specimen, crack arrest toughness data can be determined by static evaluation procedures with an accuracy which is sufficient for engineering purposes and which avoides over-conservative design.

C. Cracks under Drop Weight Loading

The impact fracture toughness K_{Id} is usually determined with precracked bend specimens in instrumented impact tests. The specimens are loaded by a drop weight or by a pendulum type impact tester. Strain gages at the tup of the striking hammer measure the load during impact. From the critical load at the moment of crack initiation the impact fracture toughness is derived.

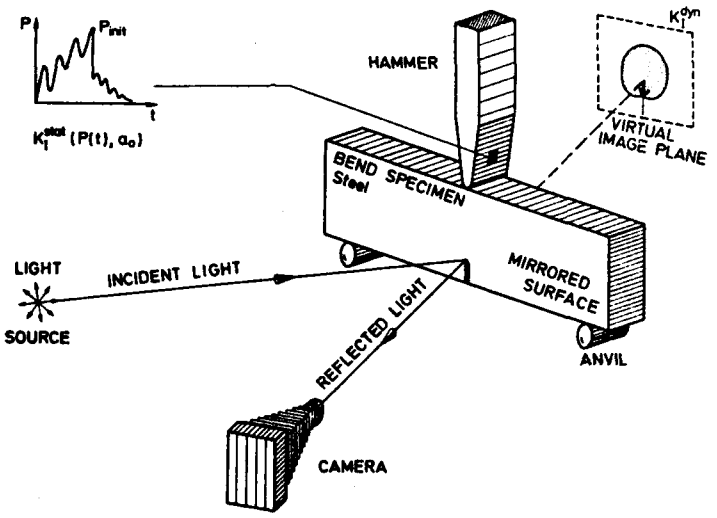

Fig. (14) - Experimental set-up for a drop weight experiment and shadow optical arrangement in reflection (schematically)

The mechanical behavior of cracks under impact loading was investigated by measuring the dynamic stress intensity factors directly at the crack tip by means of the shadow optical method of caustics [18-22]. Specimens made from the model material Araldite B and a high strength steel were investigated. Figure 14 gives a schematic view of the experimental set-up showing the shadow optical arrangement in reflection with a high strength steel specimen. The influences of dynamic effects were evaluated by comparing the dynamic stress intensity factors, K_I^{dyn}, with equivalent static stress intensity factors, K_I^{stat}. The static values were determined from the measured hammer load P_H utilizing conventional static stress intensity factor formulas from ASTM E 399.

A series of twelve shadow optical photographs of the central part of an impacted steel specimen is shown in Figure 15. Quantitative data for the two materials considered are given in Figure 16. The specimens were impacted at a velocity of 0.5 m/s by a hammer with a mass of 30 kg or 90 kg respectively. The dynamic stress intensity factors K_I^{dyn} (experimental

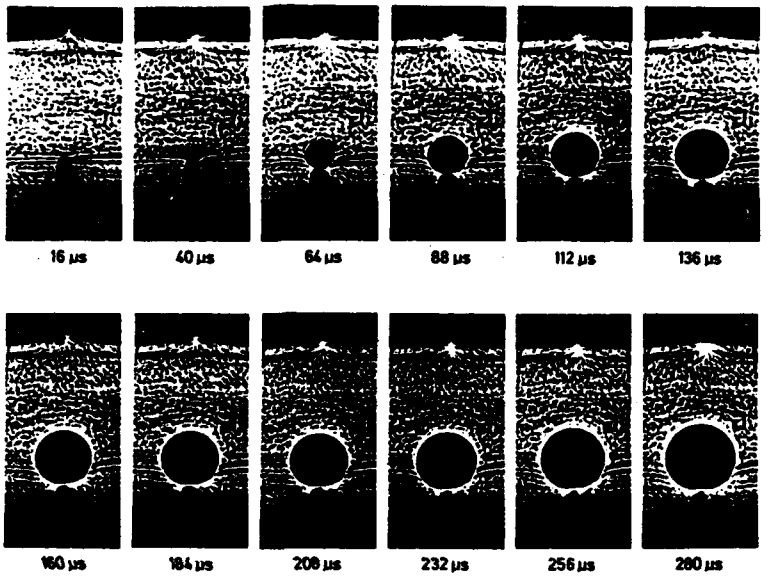

Fig. (15) - Shadow optical photographs of a precracked bend specimen during drop weight loading (photographed in reflection with a high strength steel specimen)

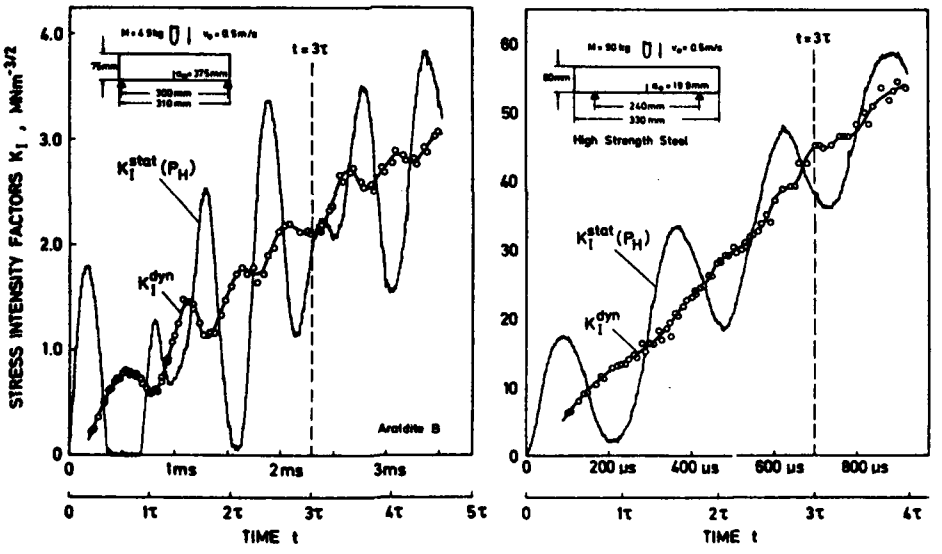

Fig. (16) - Stress intensity factors for cracks under drop weight loading a) Araldite B specimen, b) high strength steel specimen

points) and the corresponding static stress intensity factors K^{stat} (thin curves) are plotted as functions of time. The times are given in absolute units and also in relative units by normalization with the period τ of the eigen-oscillation of the impacted specimen.

The K_I^{stat}-values show a strongly oscillating behavior, whereas the actual dynamic stress intensity factors K_I^{dyn} show a more steadily increasing tendency. In the small time range, $t < \tau$, these differences are very pronounced. The differences become smaller with increasing time, but even for times larger than 3τ the influences of dynamic effects obviously have not vanished and there are still marked differences between K_I^{stat} and K_I^{dyn}. Due to a different contact stiffness the effects are larger with Araldite B specimens then with high strength steel specimens.

The behavior of specimens under impact loading was further investigated by also measuring the specimen reaction at the anvils [21]. Figure 17 compares the load measured at the striking hammer (a), the stress intensity factor measured at the crack tip (b), the load measured at the anvils (c), and the position of the specimen ends with regard to the anvils (d). The data were obtained with Araldite B specimens impacted at 1 m/s. The

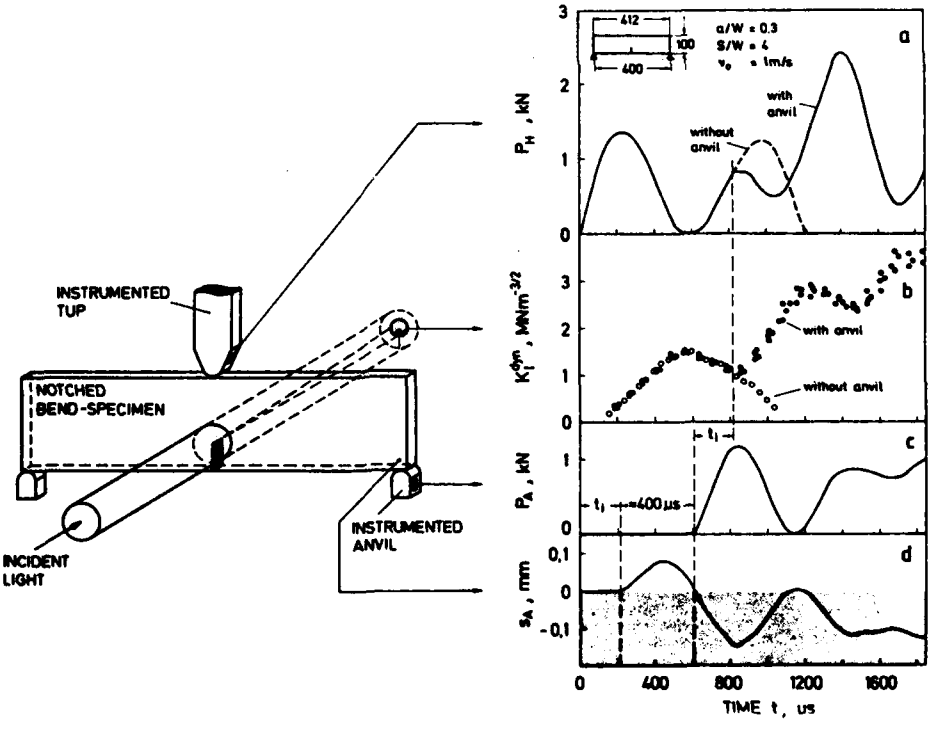

Fig. (17) - Mechanical response of a prenotched bend specimen to drop weight loading

τ-value of the specimens utilized for these investigations is about 700 µs. A comparison of the four signals indicates that non-zero loads at the anvils were registered only after a rather long time of about 600 µs. This time is about three times larger then the time it would take the slowest wave, i.e. a transverse wave, to travel from the point of impact to the anvils. This unexpected behavior is explained by diagram (d) in Figure 17. A loss of contact is observed between the specimen ends and the anvils. The loss of contact starts at about 200 µs. This time is in agreement with the above consideration of wave propagation times. For about 400 µs the specimen is completely free and only after this time, i.e. at a time of about 600 µs total, the specimen ends come into contact with the anvils. In accordance with this observation, load values are then recorded at the anvils. With different test conditions this loss of contact can occur later for a second time and loss of contact can also take place between the hammer and the specimen. These processes are illustrated in the

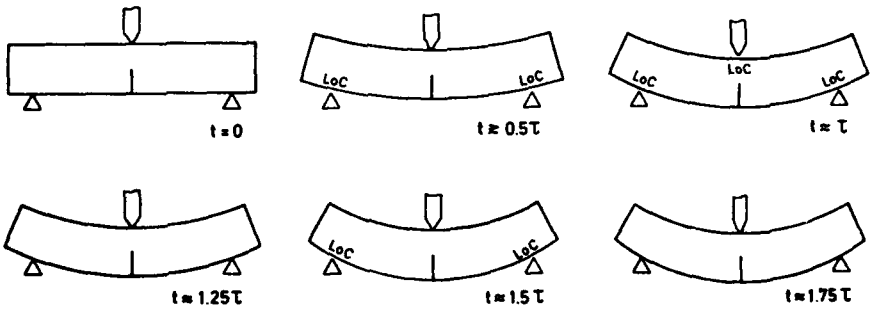

Fig. (18) - Loss of contact effects observed with prenotched bend specimens under drop weight loading

schematic representation of Figure 18. Since in the reported experiments the anvils obviously were of no influence during the early phase of the impact process, additional experiments have been performed with unsupported specimens. The results are represented by the dashed curve and open data points in Figure 17. In accordance with speculation, the early specimen reaction ($t < \tau$) is the same for both, the supported and the unsupported specimen.

The measured data demonstrate the strong influence of dynamic effects on the mechanical behavior of cracks under impact loading. A method [23] proposed to ASTM for measuring the dynamic fracture toughness value K_{Id} in instrumented impact tests assumes that for times larger than 3τ K_I^{stat}-values would represent a good approximation of the actual dynamic stress intensity factor K_I^{dyn}. However, data from the presented experiments indicate that a static analysis is not adequate to describe the loading condition in the specimen under the proposed conditions except at

much later times during the event. Very large times to fracture, however, cannot always be achieved [19]: in principle, the time to fracture is increased if the test temperature is increased and if the impact velocity is reduced. The τ-value of a specimen, on the other hand, is reduced when the specimen dimensions are reduced. Often both goals cannot simultaniously be reached due to size requirements which in general demand large specimen dimensions for high test temperatures. The conditions of course become very unfavorable for testing of brittle materials at high impact velocities [19]. Consequently the determination of reliable impact fracture toughness data with freedom of choice of test conditions requires a fully dynamic evaluation procedure.

At IWM, therefore, the dynamic concept of impact response curves has been developed [24]. The principle of the measuring procedure is illustrated in Figure 19. For fixed test conditions (i.e. specimen geometry,

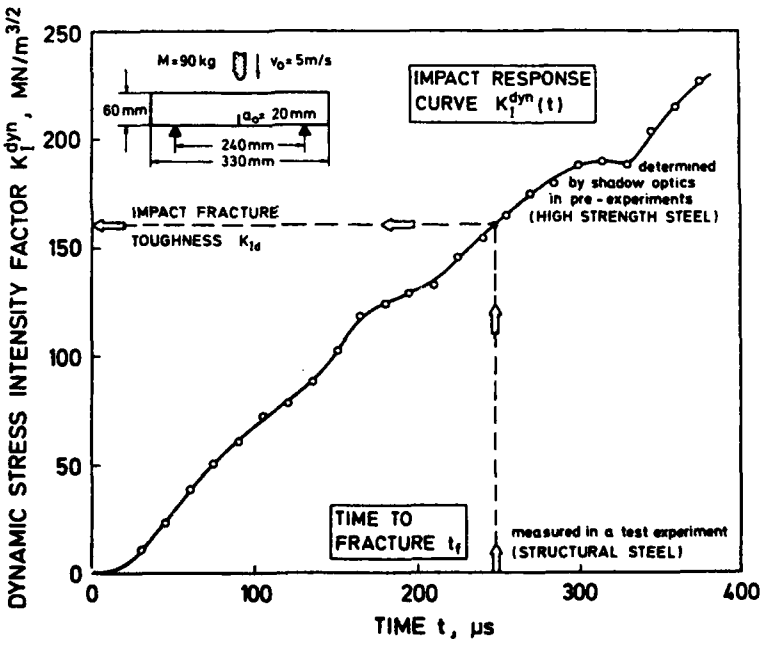

Fig. (19) - The concept of impact response curves for measuring the impact fracture toughness K_{Id}

hammer mass, impact velocity, etc.) the dynamic stress intensity factor versus time relationship is determined in a pre-experiment by means of the shadow optical method of caustics with an edge notched high strength steel specimen (see also Figure 14). The obtained curve, $K_I^{dyn}(t)$, describes the response of the specimen to the impact process. This curve, called impact response curve, is controlled by the elastic properties of the system

only. It therefore applies for all steels provided the conditions for small scale yielding are fulfilled. In the real test-experiment a precracked specimens of the steel to be investigated is then tested under the same impact conditions. In this experiment only the time to fracture is measured (e.g. by an uncalibrated strain gage near the crack tip.) This time together with the preestablished impact response curve determines the impact fracture toughness value K_{Id}.

The applicability of the measuring procedure has been checked under different test conditions. Figure 20 gives impact response curves for specimens of different sizes and different ratios of specimen length to sup-

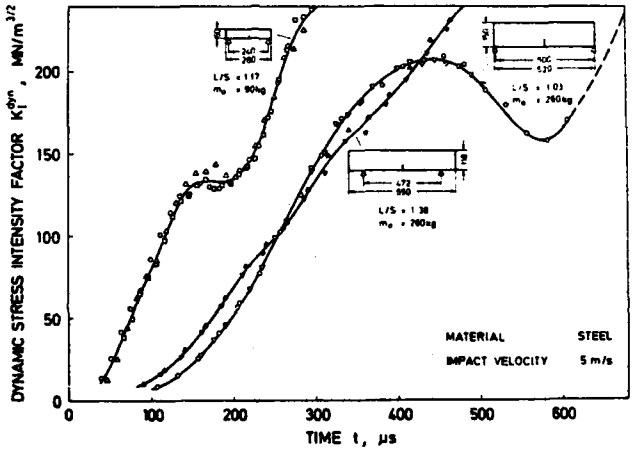

Fig. (20) - Impact response curves

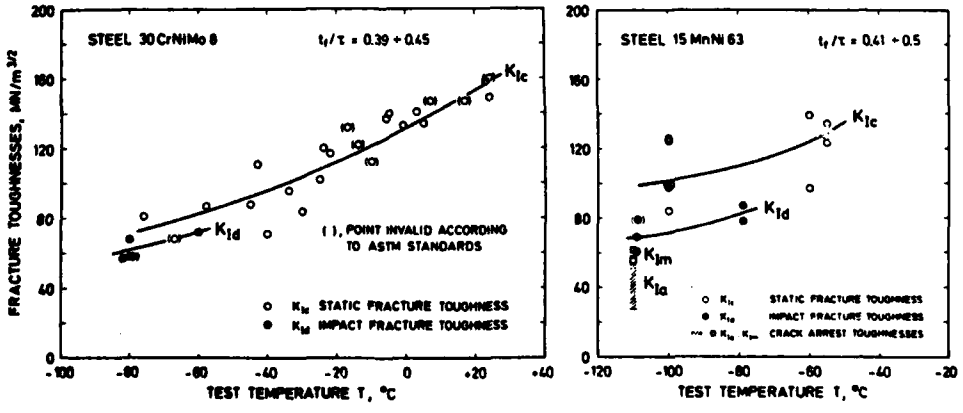

Fig. (21) - Impact fracture toughness data

port span. The specimens were impacted by a hammer of 90 kg or 260 kg at a velocity of 5 m/s. Specimens which were supported at the very ends of the specimen show a more oscillatory $K_I^{dyn}(t)$-curve. Specimens with a length to support span ratio L/S = 55/40 (as with Charpy specimens) are characterized by a more steadily increasing curve (see also [21]). Impact fracture toughness values K_{Id} determined from these response curves are shown in Figure 21 for the steels 30 CrNiMo 8 and 15 MnNi 63. A comparison with other fracture toughness data indicates that the measured values are reasonable [24]. This is not trivial since the specimens failed at relatively small times to fracture, $t_f < \bar{\tau}$, i.e. at times where the conventional procedure [23] would not be applicable.

Because of the very short times to fracture obtained in these experiments the anvils could not have influenced the specimen reaction. Since at higher loading rates the specimens would fail even earlier, it is natural that a high rate impact test (> 5 m/s) for measuring K_{Id}-values can be carried out with unsupported specimens. This loading arrangement is called "one-point-bend" loading.

Typical results of "one-point-bend" experiments [22] are shown in Figures 22 and 23. Steel specimens 270 mm long and 50 mm wide were utilized in these experiments. Impact loading was achieved by a projectile of 1.9 kg mass which was accelerated by a gas gun to a velocity of 17 m/s. The resulting impact response curve is shown in Figure 22. The stress in-

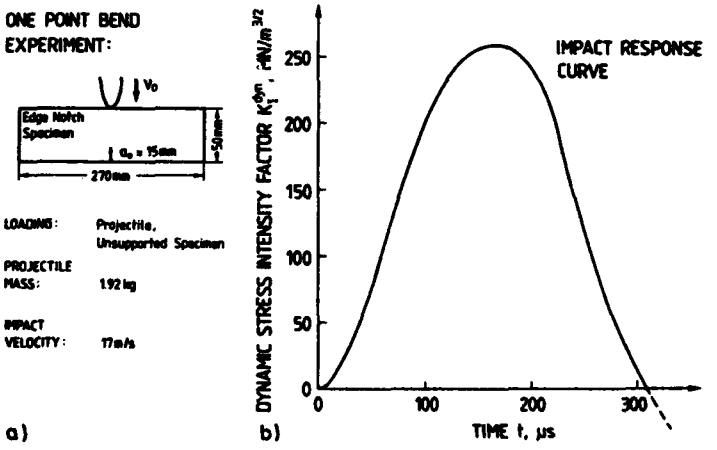

Fig. (22) - One-point-bend technique, a) test conditions, b) impact response curve

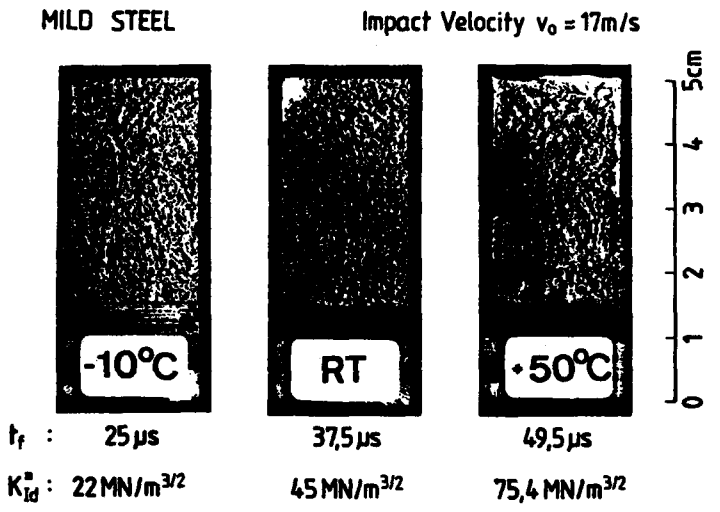

Fig. (23) - Fracture behavior under one-point-bend loading

tensity factor capacity of the loading arrangement is about 260 MN/m$^{3/2}$. Fracture toughness measurements have been performed under the same impact conditions with specimens made from a mild steel. Specimens of 20 mm thickness with sharp initial notches were tested at different temperatures. Complete failure of the specimens was observed in all experiments. Figure 23 shows the fracture surfaces of the broken specimens, the times to fracture t_f, and the resulting dynamic fracture toughness values K_{Id}. These data demonstrate the feasibility of the one-point-bend technique for measuring impact fracture toughness data at high loading rates.

Similar experiments have been performed at a lower impact velocity of 5 m/s with a pendulum type impact tester [22]. The test device was slightly modified to load unsupported specimens. At lower temperatures the specimens broke completely in spite of the only modest impact velocity.

It is evident that a quasistatic evaluation procedure would not be able to describe these experiments. The fully dynamic method of impact response curves, however, can successfully be applied even under these highly dynamic test conditions.

D. Short Pulse Loading of Cracks

High rate material data are measured under stress wave loading, e.g. achieved by projectile impact. The resulting stress pulses in general are

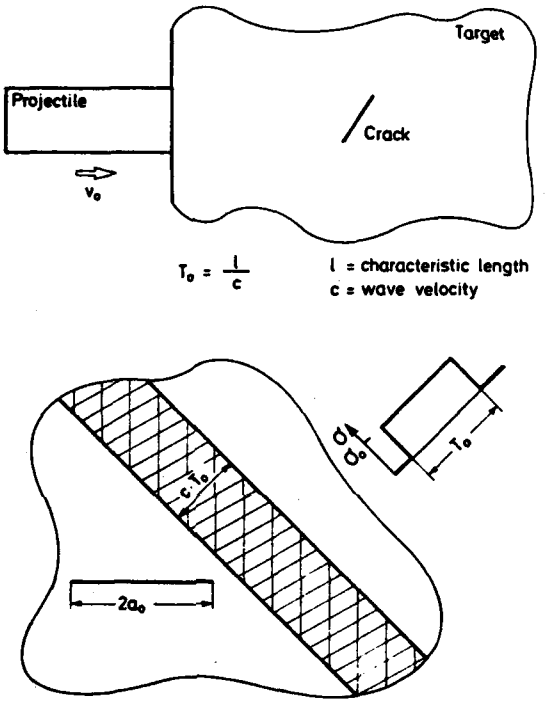

Fig. (24) - Short pulse loading of cracks

of short duration. When a specimen is hit by a projectile, compressive stress waves are generated during the impact process which propagate into the specimen and into the projectile as well. These compressive stress pulses, after reflection at the finite boundaries, load the specimen in tension. The duration of the tensile stress pulse T_0 is determined by the geometric conditions and is usually given in the form l/c, where c is a wave propagation velocity and l is a characteristic dimension, for example the length of the projectile. The amplitude of the stress pulse is controlled by the impact velocity. Thus, by varying the projectile-specimen-dimensions and the impact velocity controlled stress pulses of known duration and amplitude can be produced (see Figure 24). For experimental details see for example Shockey et al. [25,26].

Applying projectile impact techniques, Homma, Kalthoff, Shockey [26-29] studied the fracture behavior of cracks which were loaded by stress pulses of durations which are comparable or even smaller than the time it takes waves to travel the distance given by the crack length.

According to the static fracture mechanics concept, critical stresses for instability should continuously decrease with increasing crack length, as shown schematically in Figure 25. Instability stresses for cracks of different lengths which were subjected to stress pulses of different durations are shown in Figures 26 and 27 [28,29]. The presented results were obtained with specimens made from an epoxy resin and 4340 steel. The data indicate the following behavior: For short cracks the instability stresses decrease with increasing crack length, similar as in static fracture mechanics. For cracks above a certain length, however, higher stresses are needed to bring a crack to instability than under static loading conditions. Furthermore, the instability stresses seem not to decrease with increasing crack length but to stay at the same constant level. The shorter the pulse duration the larger the instability stress and the smaller the critical crack length from which on a constant behavior is observed (see Figure 27).

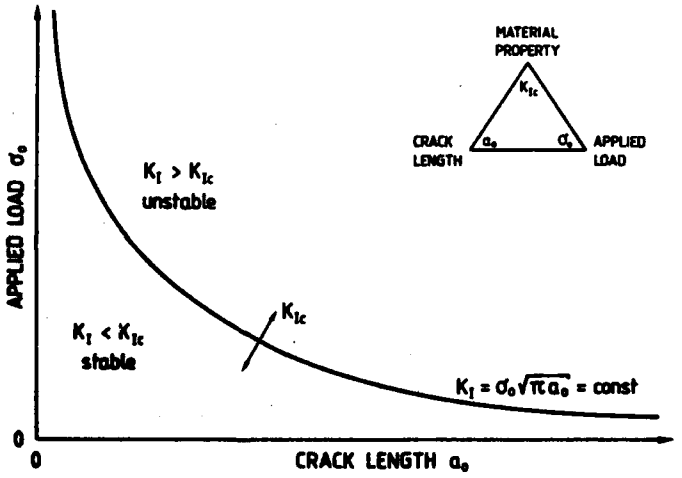

Fig. (25) - Instability behavior of cracks under static loading conditions

The observed findings demonstrate that a static instability criterion fails to describe the mechanical behavior of cracks under short lived pulses. The formal determination of fracture toughness values on the basis of static evaluation procedures would yield data which would show an increasing tendency with increasing crack length and decreasing pulse duration. Thus, the fracture criterion has to be modified to account for short duration effects.

Obviously a stress intensity factor following the simple $\sigma_0\sqrt{\pi a_0}$-relationship does not apply anymore for short pulse fracture experiments if the crack length exceeds a certain limit. The actual behavior is indeed controlled by a rather complex stress intensity factor history [27]. The principal behavior for a crack under step function load is shown in

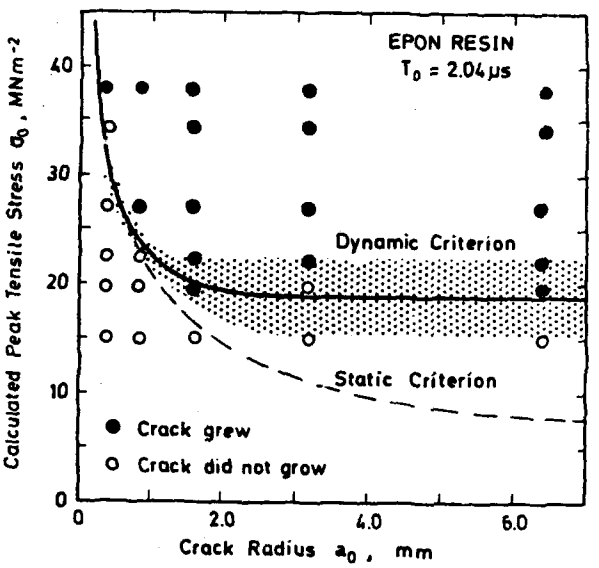

Fig. (26) - Instability stresses for cracks under short pulse loading

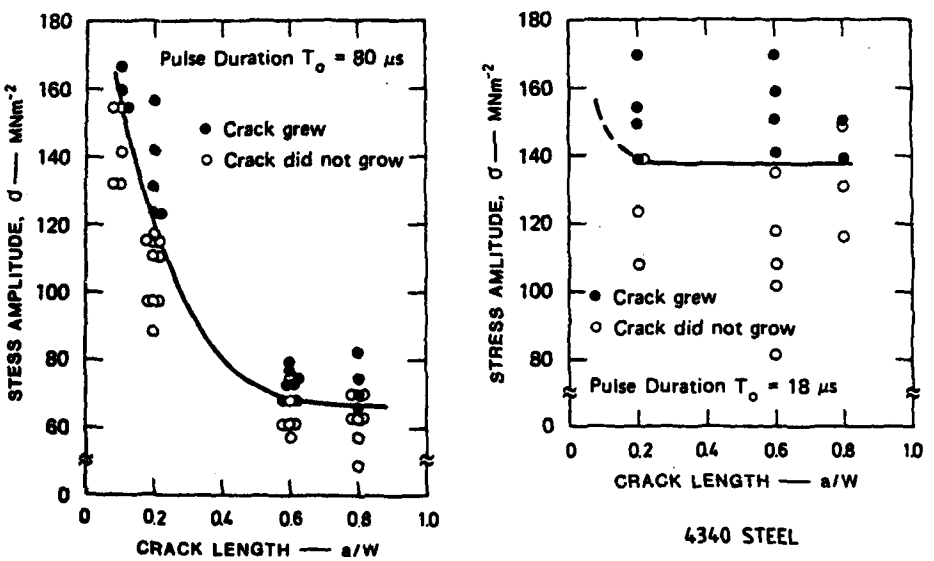

Fig. (27) - Instability stresses for cracks under short pulse loading

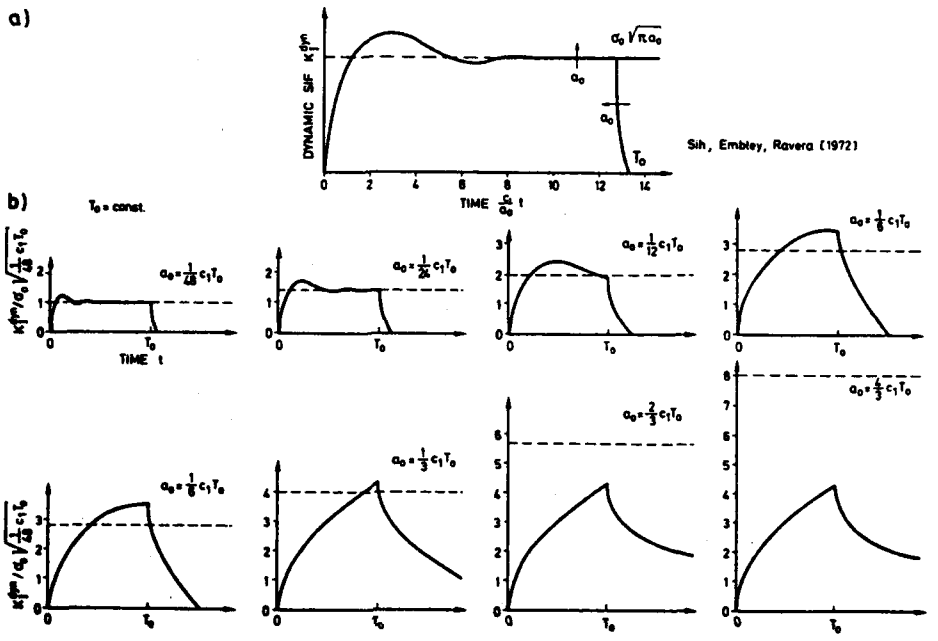

Fig. (28) - Stress intensity histories for cracks under short pulse loading

Figure 28a [30]. The dynamic stress intensity factor K_I^{dyn} is plotted as a function of the dimensionless time $(c_1/a_0)t$, where c_1 is the longitudinal wave velocity. The stress intensification first increases with time according to a square root of time relationship, overshoots the equivalent static stress intensity factor by a considerable amount, and then reaches a constant static value after damped oscillations. This behavior is plausible: For very early times, $t < a_0/c_1$, only a certain part of the crack can contribute to the stress intensification at the crack tip due to finite "information" velocities. Consequently, not the real crack length a_0 but an effective crack length a_{eff}, with $a_{eff} = ct < a_0$, determines the stress intensity factor $K_I^{dyn} = \sigma_0\sqrt{\pi a_{eff}} = \sigma_0\sqrt{\pi ct}$, where c is the "information velocity", i.e. an average wave propagation velocity. After the waves have traveled several times along the crack, $t > 10a_0/c_1$, a static situation is reached and the real crack length a_0 determines the stress intensification, $K_I^{dyn} = \sigma_0\sqrt{\pi a_0}$.

Based on these results, the stress intensity histories were derived for cracks of increasing lengths subjected to a rectangular stress pulse of finite duration T_0 [27]. The results are shown in Figure 28b. The dynamic stress intensity factors, K_I^{dyn} (full curves), are compared to the equivalent static stress intensity factors, K_I^{stat} (dashed lines). For convenience the crack lengths a_0 are measured in units c_1T_0. For short cracks, $a_0 \leq c_1T_0/30$, the stress intensity history is characterized

by an almost rectangular shape and the effective dynamic stress intensity factor is the same as the equivalent static stress intensity factor value,

$$K_{I,eff}^{dyn} = K_I^{stat} \qquad \text{for} \quad a_0 \leq c_1 T_0/30. \tag{2}$$

With increasing crack length the stress intensification becomes larger and more triangular in shape, but the average dynamic stress intensity factor becomes smaller than the equivalent static stress intensity factor value. For even larger crack lengths, $a_0 > c_1 T_0/2$, the dynamic stress intensification does not increase anymore but stays the same although the crack length and accordingly the static stress intensity factor increases. In this regime the dynamic stress intensity factor is controlled by the effective crack length $a_{eff} < a_0$, and

$$K_{I,eff}^{dyn} = \text{const} < K_I^{stat} \quad \text{for} \quad a_0 \geq c_1 T_0/2. \tag{3}$$

Based on these stress intensity considerations and the assumption that the crack has to experience a supercritical stress intensity factor for at least a certain minimum time in order to become unstable, the instability behavior was predicted [27]. Results for cracks of different length a_0, loaded by stress pulses of different amplitude σ_0, and duration T_0, are shown in a three-dimensional (σ_0-a_0-T_0)-diagram in Figure 29. The short pulse fracture behavior is represented in the rear right section of the diagram, the front left regime (long pulse durations, short crack lengths) shows the usual static behavior. For constant pulse durations and cracks above a certain length, $a_0 \geq c_1 T_0/30$, higher critical stresses are predicted than in the

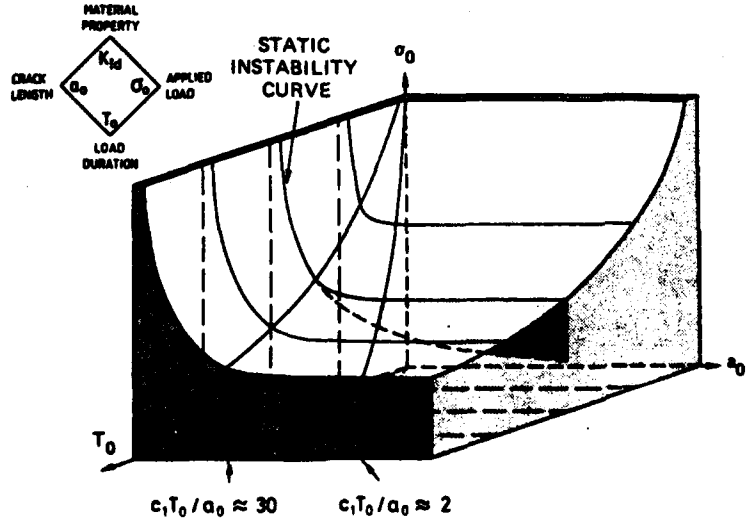

Fig. (29) - Surface of dynamic instability stresses for cracks under short pulse loading

equivalent static case. Furthermore, for crack length $a_0 \geq c_1 T_0/2$ the predicted instability stresses do not depend on crack length anymore. These theoretical predictions are in good agreement with the experimental observations.

The reported findings demonstrate the validity of the developed short pulse fracture criterion. The criterion shows the limitations of static fracture mechanics approaches and represents an appropriate basis for determining high rate fracture toughness data from short pulse fracture experiments.

ELECTRONIC ASPECTS

If time dependent mechanical quantities of any kind are measured by electronic systems the frequency response of the measuring system has to be adequate. This requirement is trivial. Very often, however, it is not sufficiently fullfilled since high frequency reactions in the mechanical test system are excited which at first are not expected.

Figures 30 and 31 give examples of insufficiently chosen frequency responses. Charpy specimens made from structural steels were impacted in an instrumented pendulum type impact tester [31,32]. The load signal from the strain gage at the tup of the striking hammer was recorded with a dual trace oscilloscope, one channel used in a high frequency mode (5 MHz or

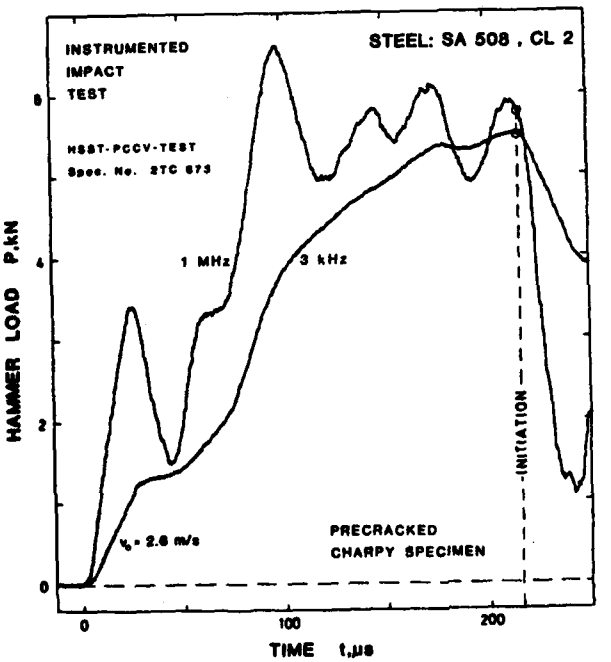

Fig. (30) - Load signal from an instrumented impact test recorded with different electronic systems (precracked Charpy specimen)

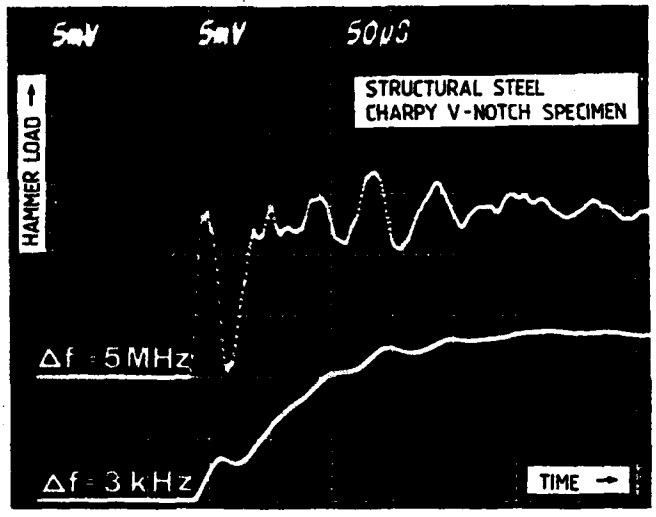

Fig. (31) - Load signal from an instrumented impact test recorded with different electronic systems (Charpy V-notch specimen)

1 MHz), the other in a 3 kHz mode. The latter band width is close to a minimum band width which is recommended in a test procedure [23] for measuring the dynamic fracture toughness with precracked Charpy specimens.

In both experiments the signal obtained from the fast channel shows a strong high frequency mechanical behavior of the specimen which is not recorded by the 3 kHz signal. Furthermore, the mean load lines of the two signals, i.e. the average curve through the signals neglecting the oscillations, are different in particular at early times. For example at 160 µs the 3 kHz signal yields a value which is about 10% to 20% too low.

Inadaequate electronic systems therefore can disturb or surpress important details of the actual mechanical behavior. Consequently erroneous material data can result. Unfortunately, human nature often tends to consider the more smooth and easy to evaluate load traces obtained from insufficient systems as more reliable and better then strongly oscillating recordings. This psychological argument however should not be the guide line for the assessment of the reliability of data.

It is preferable therefore to utilize electronic systems with a high frequency response, since erroneous data can only result if the frequency response is too low but not if it is too high.

SUMMARY AND CONCLUSION

Influences of time effects on test procedures for measuring dynamic material strength values have been analyzed. In particular, procedures for measuring the crack arrest toughness and the initiation fracture toughness at high loading rates have been considered. It is shown, that time effects

can have a strong influence on the mechanical behavior of the cracks. For cracks at arrest the stress condition at the crack tip is still dynamic and not static, although the crack velocity is zero at the moment of arrest. Cracks under drop weight loading, in general, cannot be adequately described on the basis of quasistatic analyses. Static criteria also fail to describe the instability behavior of cracks under short pulse loading. Dynamic material properties based on static evaluation procedures, therefore, can be erroneous. It is further demonstrated that important details of the mechanical behavior of cracks can be distorted or surpressed if the frequency response of the electronic measuring system is not adequate. A reliable determination of material strength data, therefore, requires the consideration of dynamic effects on both the mechanical and the electronic aspects of the measuring procedure. Techniques which take the influences of dynamic effects into account in an appropriate form have been outlined: i.e. the reduced dynamic effects crack arrest specimen, the dynamic concept of impact response curves and the short pulse fracture mechanics concept.

Fully dynamic procedures for measuring dynamic material properties in general are more sophisticated and more complicated than for measuring static material properties. This however is unvoidable and a necessary consequence of the fact that A DYNAMIC EXPERIMENT IS MORE THAN A FAST STATIC EXPERIMENT.

REFERENCES

[1] Manogg, P., "Anwendung der Schattenoptik zur Untersuchung des Zerreißvorgangs von Platten", Dissertation, Universität Freiburg, Germany, 1964.

[2] Manogg, P., "Schattenoptische Messung der spezifischen Bruchenergie während des Bruchvorgangs bei Plexiglas", Proc. Int. Conf. Physics of Non-Crystalline Solids, Delft, The Netherlands, pp. 481-490, 1964.

[3] Theocaris, P. S., "Local Yielding Around a Crack Tip in Plexiglas", J. Appl. Mech., Vol. 37, pp. 409-415, 1970.

[4] Beinert, J., and Kalthoff, J. F., "Experimental Determination of Dynamic Stress Intensity Factors by Shadow Patterns" in Mechanics of Fracture, Vol. 7, Ed. G.C. Sih, Martinus Nijhoff Publishers, The Hague, Boston, London, pp. 281-330, 1981.

[5] Kalthoff, J. F., "Stress Intensity Factor Determination by Caustics", Int. Conf. Experimental Mechanics, Society for Experimental Stress Analysis and Japan Society of Mechanical Engineers, Honolulu-Maui, Hawaii, U.S.A., May 23-28, 1982.

[6] Kalthoff, J. F., "On Some Current Problems in Experimental Fracture Dynamics", Workshop on Dynamic Fracture, Ed. W.G. Knauss, California Institute of Technology, Pasadena, Calif., U.S.A., February 17-18, 1983.

[7] Kalthoff, J. F., Beinert, J., and Winkler, S., "Measurements of Dynamic Stress Intensity Factors for Fast Running and Arresting Cracks in Double-Cantilever-Beam-Specimens", ASTM STP 627 - Fast Fracture and Crack Arrest, American Society for Testing and Materials, Philadelphia, U.S.A., pp. 161-176, 1977.

[8] Kalthoff, J. F., Beinert, J., Winkler, S., and Klemm, W., "Experimental Analysis of Dynamic Effects in Different Crack Arrest Test Specimens", ASTM STP 711 - Crack Arrest Methodology and Applications, American Society for Testing and Materials, Philadelphia, U.S.A., pp. 109-127, 1980.

[9] Kalthoff, J. F., "Zur Ausbreitung und Arretierung schnell laufender Risse", Fortschritt-Berichte der VDI-Zeitschriften, Reihe 18, Nr. 4, VDI-Verlag, Düsseldorf, 1978.

[10] Kalthoff, J. F., Beinert, J., and Winkler, S., "Influence of Dynamic Effects on Crack Arrest", Final Report prepared for Electric Power Research Institute, Palo Alto, Calif., under Contract No. RP 1022-1, IWM-Report W 4/80, Fraunhofer-Institut für Werkstoffmechanik, 7800 Freiburg, West-Germany, 1980.

[11] Crosley, P. B., and Ripling, E. J., "Crack Arrest Toughness of Pressure Vessel Steels", Nuclear Engineering and Design, Vol. 17, No. 1, pp. 32-45, August 1971.

[12] Crosley, P. B., and Ripling, E. J., "Towards Development of a Standard Test for Measuring K_{Ia}", ASTM STP 627 - Fast Fracture and Crack Arrest, American Society for Testing and Materials, Philadelphia, U.S.A., pp. 372-391, 1977.

[13] Hahn, G. T., Hoagland, R. G., Kanninen, M. F., and Rosenfield, A. R., "A Preliminary Study of Fast Fracture and Arrest in the DCB Test Specimen", Proc. Int. Conf. Dynamic Crack Propagation, Ed. G.C. Sih, Lehigh University, Bethlehem, Pa., U.S.A., July 10-12, 1972.

[14] Hahn, G. T., Gehlen, P. C., Hoagland, R. G., Kanninen, M. F., Popelar, C., Rosenfield, A. R., et al., "Critical Experiments, Measurements and Analyses to Establish a Crack Arrest Methodology for Nuclear Pressure Vessel Steels", BMI-1937, 1959, 1995, Battelle Columbus Laboratories, Columbus, Ohio, Aug. 1975, Oct. 1976, May 1978.

[15] Beinert, J., Klemm, W., and Kalthoff, J. F., "Mechanik und Stoffverhalten bei der Arretierung von Rissen", IWM-Report V 16/83, pepared for European Community on Steel and Coal, under Contract No. 7210.Ke 107, Fraunhofer-Insitut für Werkstoffmechanik, 7800 Freiburg, West-Germany, April 1983.

[16] Kalthoff, J. F., Beinert, J., and Winkler, S., "Einfluß dynamischer Effekte auf die Bestimmung von Rißarrestzähigkeiten und auf die Anwendung von Rißarrestsicherheitsanalysen", 9. Sitzung, Arbeitskreis Bruchvorgänge im Deutschen Verband für Materialprüfung, Köln, Germany, Oct. 6-7, 1976.

[17] Beinert, J., and Kalthoff, J. F., "The Development of a Crack Arrest Test Specimen with Reduced Dynamic Effects", this publication.

[18] Kalthoff, J. F., Winkler, S., and Beinert, J., "The Influence of Dynamic Effects in Impact Testing", Int. Journ. of Fracture, Vol. 13, pp. 528-531, 1979.

[19] Kalthoff, J. F., Böhme, W., Winkler, S., and Klemm, W., "Measurements of Dynamic Stress Intensity Factors in Impacted Bend Specimens", CSNI Specialist Meeting on Instrumented Precracked Charpy Testing, EPRI, Palo Alto, Calif., U.S.A., Dec. 1-3, 1980.

[20] Kalthoff, J. F., Böhme, W., and Winkler, S., "Analysis of Impact Fracture Phenomena by Means of the Shadow Optical Method of Caustics", VIIth Int. Conf. Experimental Stress Analysis, Society for Experimental Stress Analysis, Haifa, Israel, Aug. 23-27, 1982.

[21] Böhme, W., and Kalthoff, J. F., "The Behavior of Notched Bend Specimens in Impact Testing", Int. Journ. of Fracture, Vol. 20, R139-143, 1982.

[22] Kalthoff, J. F., Winkler, S., Böhme, W., and Shockey, D.A., "Mechanical Response of Cracks to Impact Loading", Int. Conf. on Dynamic Mechanical Properties and Fracture Dynamics of Engineering Materials, Czechoslovak Academy of Sciences, Institute of Physical Metallurgy, Brno-Valtice, CSSR, June 16-18, 1983.

[23] ASTM E 24.03.03, "Proposed Standard Method of Test for Instrumented Impact Testing of Precracked Charpy Specimens of Metallic Materials", Draft 2c, American Society for Testing and Materials, Philadelphia, U.S.A., 1980.

[24] Kalthoff, J. F., Winkler, S., Böhme, W. and Klemm, W., "Determination of the Dynamic Fracture Toughness K_{Id} in Impact Tests by Means of Response Curves", 5th Int. Conf. Fracture, Cannes, March 29 - April 3, 1981, Advances in Fracture Research, Ed. D. Francois et al., Pergamon Press, Oxford, New York, 1980.

[25] Shockey, D.A., and Curran, D.R., "A Method for Measuring K_{Ic} at Very High Strain Rates", ASTM STP 536 - Progress in Flow Growth and Fracture Toughness Testing, American Society for Testing and Materials, Philadelphia, U.S.A., pp. 297-311, 1973.

[26] Shockey, D.A., Kalthoff, J. F., Homma, H., and Ehrlich, D. C., "Response of Cracks to Short Pulse Loading", Workshop on Dynamic Fracture, Ed. W.G. Knauss, California Institute of Technology, Pasadena, Calif., U.S.A., February 17-18, 1983.

[27] Kalthoff, J. F., and Shockey, D. A., "Instability of Cracks under Impulse Loads", J. Appl. Phys., Vol. 48, No. 3, pp. 986-993, March 1977.

[28] Shockey, D. A., Kalthoff, J. F., and Ehrlich, D. C., "Evaluation of Dynamic Crack Instability Criteria", Int. Journ. of Fracture, Vol. 22, pp. 217-229, 1983.

[29] Homma, H., Shockey, D. A., and Muragama, Y., "Response of Cracks in Structural Materials to Short Pulse Loads", submitted to J. Mech. Phys. Solids.

[30] Sih, G. C., Embley, G. T., and Ravera, R. J., "Impact Response of a Plane Crack in Extension", Int. Journ. Solids Structures, Vol. 8, pp. 977-993, 1982.

[31] Kalthoff, J. F., and Winkler, S., "Remarks on Instrumentation Requirements for Frequency Response", CSNI Specialists Meeting on Instrumented Precracked Charpy Testing, EPRI, Palo Alto, Calif., U.S.A., Dec. 1-3, 1980.

[32] Winkler, S., and Kalthoff, J. F., "Dynamic Precracked Charpy Evaluation Test - HSST-Program", IWM Report No. W 4/82, Fraunhofer-Institut für Werkstoffmechanik, 7800 Freiburg, West-Germany, 1982.

END

FILMED

1-84

DTIC